Journal of Physiology (1988), **406**, *pp.* 115–146
With 2 plates and 11 text-figures
Printed in Great Britain

CHANGES IN THE CALCIUM CURRENT OF RAT HEART VENTRICULAR MYOCYTES DURING DEVELOPMENT

BY NERI M. COHEN AND W. J. LEDERER

From the Department of Physiology, University of Maryland at Baltimore, School of Medicine, 660 West Redwood Street, Baltimore, MD 21201, U.S.A.

(*Received 30 June 1987*)

SUMMARY

1. Calcium current (I_{Ca}) was recorded in single rat heart cells at two periods during development: (1) at 2–7 days post-partum (neonatal), and (2) at 6–8 weeks (adult).

2. We measured both transient and steady-state components of I_{Ca} and could describe I_{Ca} in terms of the steady-state activation (d_∞) and inactivation (f_∞) parameters, the channel reversal potential ($E_{channel}$) and a relative conductance parameter, g_r.

3. In adult single cells, the application of ryanodine (10 μM), an agent known to alter the function of the sarcoplasmic reticulum (SR), abolished contraction rapidly and increased I_{Ca}. Ryanodine also produced a 13 mV shift in f_∞ towards more positive potentials and altered its slope, while producing a small increase in g_r but no effect on d_∞. In neonatal single cells, ryanodine (10 μM) had no significant effect on contraction, I_{Ca}, d_∞, f_∞, or g_r. Caffeine (10 mM), a less specific agent widely used to investigate sarcoplasmic reticulum function, had actions similar to those of ryanodine.

4. In adult myocytes, when EGTA (10 or 20 mM) or bis(*o*-aminophenoxy)ethane-*N*,*N*,*N*′,*N*′-tetraacetic acid (BAPTA, 10 mM) were included in the pipette solution, contractions were rapidly abolished, while a small (4 mV) shift of f_∞ to more positive potentials was seen. A large additional shift of f_∞ was observed when ryanodine (10 μM) was added to the superfusion solution in the continued presence of EGTA or BAPTA. The alterations of I_{Ca} in EGTA (or BAPTA) plus ryanodine were the same as those seen in ryanodine alone. In neonatal cells, in contrast, when EGTA or BAPTA were included in the pipette solution we observed only a small effect on f_∞ and the application of ryanodine had no effect.

5. Electron micrographs of our preparations show that the dissociated adult cells have sharp sarcolemmal borders, fully developed sarcomeres with T-tubules and sarcoplasmic reticulum membranes. In contrast, the neonatal cells that we use have few of these intracellular structures. Our observations in these preparations are consistent with the work of others (e.g. Penefsky, 1974; Hirakow & Gotoh, 1975; Ishikawa & Yamada, 1975; Legato, 1975; Hoerter, Mazet & Vassort, 1981).

6. Our data suggest that fully developed sarcoplasmic reticulum in rat heart cells can affect I_{Ca}. We discuss these results in terms of two possible explanations: (1) a

physical link between the sarcolemmal (SL) calcium channel and the sarcoplasmic reticulum calcium-release channel (via spanning proteins – foot processes – or linking proteins) and (2) an intracellular Ca^{2+} concentration- ($[Ca^{2+}]_i$) dependent modulation of I_{Ca}.

7. We conclude that some of the differences in I_{Ca} measured in rat heart cells during development can be attributed to the development of the sarcoplasmic reticulum and its connections to the T-tubules and sarcolemma via the spanning proteins.

INTRODUCTION

During development, calcium metabolism in rat heart appears to change significantly. Force development, for example, changes its dependence on external Ca^{2+} concentration ($[Ca^{2+}]_o$) (Bers, Philipson & Langer, 1981) and becomes less sensitive to blockade of I_{Ca} (Boucek, Shelton, Artman, Mushlin, Starnes & Olson, 1984). The intracellular source and sink of Ca^{2+}, the sarcoplasmic reticulum (SR), matures anatomically (Hoerter, Mazet & Vassort, 1981; Page & Buecker, 1981) and becomes functional (Nayler & Fassold, 1977; Fabiato, 1982; Maylie, 1982) during development. Although reduction in I_{Ca} with development would be consistent with the observed changes in contractility as well as the reported shortening of the action potential and reduction of the plateau (Langer, Brady, Tan & Serena, 1975), quantitative comparisons have not yet been made.

We have investigated the changes of I_{Ca} during development in rat heart. Our experimental results show that during development changes in I_{Ca} do indeed occur, are large, and can be correlated with the development of a normally functioning sarcoplasmic reticulum. The work also suggests that it is the functioning sarcoplasmic reticulum that brings about some of these changes.

A preliminary account of these results has been presented to the Society of General Physiologists (Cohen & Lederer, 1986).

METHODS

Single cell isolation procedures

Isolated cultured single cells were prepared from neonatal (2–7 days old) rat hearts by techniques described fully in a preceding paper (Cohen & Lederer, 1987). Briefly, the hearts were mechanically dissociated in a Ca^{2+}-free solution containing 1·0 mg/ml collagenase (type II-S; Sigma, St Louis, MO, U.S.A.) and incubated at 37 °C for 1 h. The cells were plated on cut cover-glass No. 1 (25 mm square; Corning Glass Works, Corning, NY, U.S.A.) in Dulbecco's Modified Eagle's Medium (DMEM; GIBCO, Grand Island, NY, U.S.A.) supplemented with 10 % Cadet Calf Serum (CCS; 2003 Biocell, Carson, CA, U.S.A.) in small (35 mm) tissue culture dishes (3001 Falcon, Oxnard, CA, U.S.A.) and incubated at 37 °C in a CO_2 incubator (5 % CO_2, 95 % O_2; pH 7·4) for 2 days.

Adult rats of either sex weighing 200–300 g were anaesthetized with 50 mg/kg sodium pentobarbitone and killed by cervical dislocation. The hearts were rapidly removed from the chest and perfused through the aorta and coronary circulation using a Langendorff method (constant pressure = 70 cmH_2O) with a nominally Ca^{2+}-free Tyrode solution (in mM): NaCl, 145; $NaHCO_3$, 24; KCl, 4·7; KH_2PO_4, 1; $MgSO_4$, 1; glucose, 11. After perfusion with approximately 50 ml of this solution, the heart was perfused with the same solution containing 1 mg/ml collagenase (type II; Worthington Biomedical Inc., Freehold, NJ, U.S.A.), 0·25 mg/ml hyaluronidase (type I-S; Sigma, St Louis, MO, U.S.A.) and 10 μM-$CaCl_2$, for 25–30 min. The heart was then mechanically dissociated. The resulting single cells were rod-shaped with clear striations. The cells were stored in a modified Tyrode solution containing (in mM): NaCl, 145; KCl, 4; $CaCl_2$, 1; $MgCl_2$, 1; glucose,

10; and HEPES, 10; pH 7·36 at 35–37 °C. Of the cells, at least 25–30 % were quiescent and suitable for experiments.

Experimental procedure

Cells were rapidly transferred to the experimental chamber and superfused at 1 ml/min with modified Tyrode storage solution containing 10 μM-tetrodotoxin (TTX) (Sigma, St Louis, MO, U.S.A.). Rapidly tapering pipettes were pulled (BB-CH Mechanex, Geneva, Switzerland) from borosilicate glass (1·5 mm w/fil No. 1B150F-6; World Precision Instruments Inc., New Haven, CT, U.S.A.) to a tip diameter of slightly more than 1 μm. The average electrode resistance was about 3 MΩ when filled with (in mM): potassium glutamate, 129; CsCl, 20; NaCl, 1; HEPES, 10 (pH 7·4); and EGTA, 0·01. CsCl was included in the pipette solution to block outward potassium currents. Experiments were done with 20 mM-Cs^+ in the pipette solution as noted above or 140 mM-CsCl in the pipette solution as carried out in Fig. 7, without altering our results. We did not compensate for the electrode tip potential of about 4 mV. 'Whole-cell' voltage clamp experiments (Hamill, Marty, Neher, Sakmann & Sigworth, 1981) were carried out at room temperature (21–22 °C) using a Dagan voltage clamp (feed-back resistor 0·1 or 1 GΩ; model 8900, Dagan Corp., Minneapolis, MN, U.S.A.). Pipette capacitance was compensated after formation of a gigaohm seal. After the patch was ruptured the series resistance approximately doubled and up to about 80 % of the total resistance was compensated. Action potentials (Fig. 1) were recorded in the current clamp mode (with $I = 0$); the pipette was filled with (in mM): potassium glutamate, 149; NaCl, 1; HEPES, 10 (pH 7·4); and EGTA, 0·01; and the cells superfused with a modified Tyrode solution containing (in mM): NaCl, 145; KCl, 4; $CaCl_2$, 1; $MgCl_2$, 1; glucose, 10; and HEPES, 10 (pH 7·36). Data were stored using an FM tape-recorder (Model D, A. R. Vetter Co., Rebersburg, PA, U.S.A.) or a video tape-recorder (VCR7200, Sanyo Corp., Tokyo, Japan) and a modified digital processor (PCM-501ES, Sony Corporation of America, Park Ridge, NJ, U.S.A; modified by Unitrade Inc. Philadelphia, PA, U.S.A; cf. Bezanilla, 1985).

In the experiments described in Figs 4 and 7, contraction was measured off-line as cell shortening using a video edge tracking system (Instruments for Physiology and Medicine, San Diego, CA, U.S.A.) and recorded video images of the contracting cell.

Electron microscopy

Isolated adult and neonatal myocytes were submersion-fixed overnight in 4 parts formaldehyde: 1 part glutaraldehyde (v/v) cacodylate-buffered isosmolal fixative according to McDowell & Trump (1976) and then transferred to buffer. The tissue was washed in buffer for 1 h and then dehydrated in a series of ethyl alcohols in rising concentrations, transferred to propylene oxide and embedded in polybed-812 embedding media. Blocks of each specimen were selected for thin sections and cut using a Dupont Ultra Microtome. The sections were double stained with uranyl acetate and lead citrate for 30 min and then examined in a JEOL-100B Electron Microscope using low and high magnification. From each section only images that included intact cells with complete sarcolemma were reviewed. Our particular focus was on the plasma membrane and on the sarcoplasmic reticulum.

Curve-fitting procedure

Data was analysed off-line using software described previously (Cohen & Lederer, 1987). Records of membrane current were fitted by a non-linear least-squares method to a single exponential equation:

$$I(t) = \{A[\exp(-t/\tau)] + \text{offset}\}. \quad (1)$$

The amplitude (A) of I_{Ca} was estimated at $t = 0$ and the time constant of decay by τ. The data for the steady-state kinetic parameters was analysed using the same fitting procedure as above to a Boltzmann equation:

$$d_\infty = [1 + \exp(-(V - V_h)/k)]^{-1}, \quad (2)$$

$$f_\infty = [1 + \exp((V - V_h)/k)]^{-1}. \quad (3)$$

Neither V_h nor k (for d_∞ or f_∞) was sensitive to various methods used to estimate $I(0)$ and τ was minimally affected, as discussed previously (Cohen & Lederer, 1987). Consequently, we continued to use eqn (1) and a monoexponential fit of I_{Ca} records and tail currents to estimate $I(0)$ and τ.

RESULTS

Action potential

Action potentials from the briefly cultured neonatal rat heart cells and adult ventricular myocytes recorded by us are similar to action potentials previously reported (Langer *et al.* 1975; van Ginneken & Jongsma, 1983; Mitchell, Powell, Terrar & Twist, 1984; Cohen & Lederer, 1987). In neonatal ventricular myocytes, the plateau is prominent in contrast to the more rapidly repolarizing action potential of adult rat heart cells as shown in Fig. 1. We have investigated the developmental

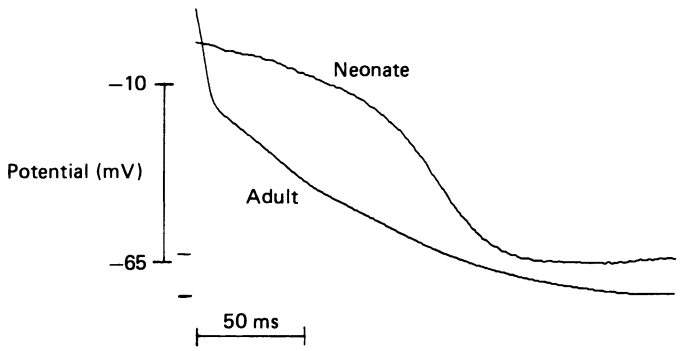

Fig. 1. Action potential records from isolated neonatal and adult single heart cells. Action potentials were recorded from adult single ventricular myocytes or single cultured neonatal cells after a 1 ms stimulus under control conditions applied using the single current clamp electrode. Lines indicating pre-stimulation membrane potentials have been drawn: adult, −76 mV; neonate, −63 mV. Control solutions were used (no TTX in superfusion solution, no Cs^+ in pipette solution). Stimulus rate, 0·5 Hz; temperature, 21–22 °C.

changes in I_{Ca} to determine if changes in I_{Ca} could be responsible, in part, for the changes in action potential shape that are observed. In this study we have not investigated the roles of other current components in the changes of action potential shape during development. Since I_{Ca} inactivates rapidly at plateau potentials in both adult and neonatal rat heart cells (Isenberg & Klockner, 1982; van Ginneken & Jongsma, 1983; Cohen & Lederer, 1987), the transient component of I_{Ca} is unlikely to account for these age-related differences. Therefore, the differences in the steady-state component of I_{Ca} (the calcium 'window' current, cf. van Ginneken & Jongsma, 1983; Cohen & Lederer, 1987) and the differences in steady-state variables d_∞ and f_∞ between neonatal and adult cells were examined.

Calcium current (I_{Ca})

Figure 2 shows the results of experiments measuring calcium channel current from both neonatal and adult myocytes with Ca^{2+} as the principal charge carrier. In order to examine only the role of 'L'-type calcium channels in 'whole-cell' current records, the holding potential of −50 mV was chosen (Nilius, Hess, Lansman & Tsien, 1985). Depolarizing pulses of 200 ms duration to 0 mV were applied at 0·5 Hz. There are several features of I_{Ca} evident in Fig. 2*A* that can be noted. The density of I_{Ca} in

neonatal cells is larger than that seen in the adult. The surface area, estimated by means of measurements of electrical capacitance, is generally about 2–3 times less in neonatal cells than in adult cells. Similarly the steady-state I_{Ca} at the end of the 200 ms depolarizing pulse is greater in neonatal cells. Consistent with this finding is the larger tail current observed in neonatal cells on repolarization. The transient and steady-state components of I_{Ca} and the tail currents are abolished by 0·1 mM-Cd^{2+} applied extracellularly in both neonatal and adult cells. Figure 2*B* and *C* shows data that were obtained by stepping the membrane potential briefly (10 ms) to −90 mV and then to various test potentials (V_{test}) for 200 ms once every 2 s. Depolarization to V_{test} elicited no phasic current at potentials negative to −40 mV. Between −40 and +55 mV the depolarization led to an inward I_{Ca} which was largest at 0 mV. In neonatal cells the time constant of I_{Ca} inactivation (τ) was relatively constant at about 10 ms for V_{test} between −40 and 0 mV. In adult cells, however, τ was larger, declining from nearly 30 ms at −40 mV to about 10 ms at 0 mV. For V_{test} of +5 to +60 mV the time constant of inactivation was larger for neonatal cells than for adult cells. In neonatal cells it increased from 10 ms at 0 mV to about 75 ms at +55 mV. In adult cells τ increased from 10 ms at 0 mV to only about 30 ms at +55 mV. The inward Cd^{2+}-sensitive transient component of I_{Ca} became outward at about +55 mV, a value similar to that reported for both adult and neonatal cells (Lee & Tsien, 1982; Cohen & Lederer, 1987).

Figure 2*D* shows the steady state current–voltage relationships measured at the end of 200 ms voltage clamp pulses. From the holding potential of −50 mV, 200 ms depolarizing voltage clamp pulses to test potentials were applied at 0·5 Hz. Cadmium (0·1 mM) was then added to block I_{Ca}. The difference between the current records in the presence and absence of Cd^{2+} is the Cd^{2+}-sensitive current shown as the data points in Fig. 3*E*. This presumably represents the steady-state component of I_{Ca}, the calcium channel 'window current'.

When compared to adult cells, the larger transient and steady-state components of I_{Ca} seen in the neonatal cells may reflect a greater calcium channel density in the neonatal cells, although we have no direct information on this point. These differences could also reflect other differences in calcium channel current properties of neonatal cells *vs.* adult cells. This possibility was suggested by the differences in the voltage dependence of the time constant of inactivation of I_{Ca} in adult *vs.* neonatal cells and is examined below.

Steady-state kinetic parameters (d_∞ and f_∞)

To investigate the properties of the steady-state component of I_{Ca} observed in Fig. 2 we measured steady-state activation (d_∞) and steady-state inactivation (f_∞) and the results are displayed in Fig. 3.

To investigate d_∞, the membrane potential was held at −50 mV and 10 ms pulses to various V_{test} were imposed at 0·5 Hz. The tail current (I_{test}) was measured on returning to the holding potential following V_{test} in the presence and absence of 0·1 mM-Cd^{2+}. Two original record examples are shown in Fig. 3*A* at V_{test} of −15 mV (left panel) and at +30 mV (right panel). The lower traces represent I_{Ca}, the Cd^{2+}-subtracted records (points), and the monoexponential fits (continuous lines) as described in the Methods section. In order to control for I_{Ca} 'run-down' (Byerly &

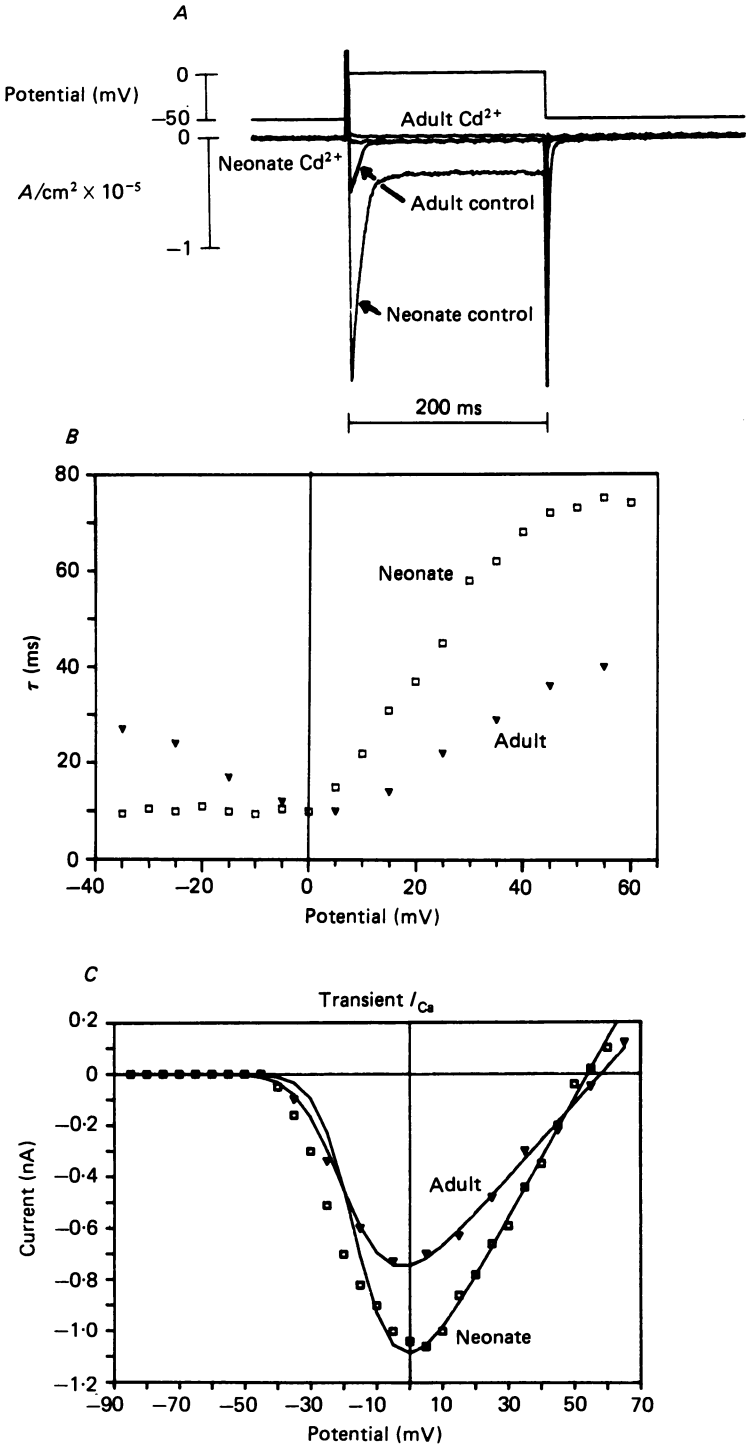

Fig. 2 *A–C*. For legend see facing page.

Hagiwara, 1982; Fenwick, Marty & Neher, 1982; Bean, 1984; Lee & Tsien, 1984), all trials to V_{test} were alternated with trials to V_{test}^{max} (the test potential that gives the largest tail current) and the ratio of the resulting tail currents (I_{test}/I_{test}^{max}) was determined and plotted in Fig. 3*B*. The smooth curve shows the best-fit line described by eqn (2) (neonatal constants: $V_h = -2{\cdot}9$ mV, $k = 6{\cdot}85$ mV; adult constants: $V_h = -1{\cdot}1$ mV, $k = 8{\cdot}01$ mV).

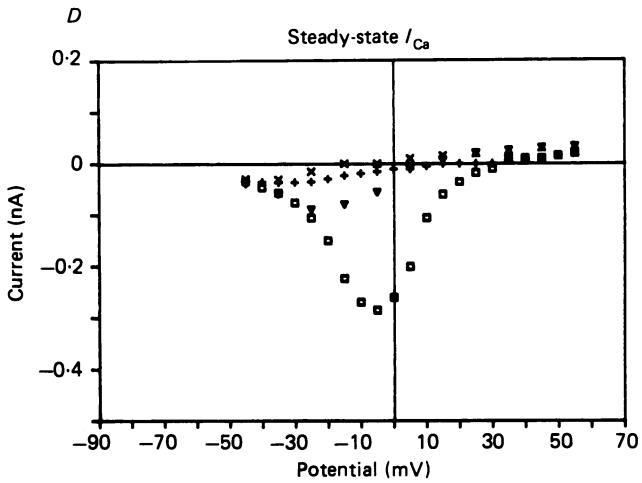

Fig. 2. Calcium current (I_{Ca}) in neonatal and adult rat heart cells normalized to surface area. *A*, current density for adult and neonatal heart cells elicited by 200 ms depolarizing pulses to 0 mV from the holding potential (−50 mV). In each preparation 0·1 mM-$CdCl_2$ was subsequently added to the superfusion solution to block I_{Ca} and the resulting records are shown. In panels *B* and *C* the membrane potential was stepped to −90 mV for 10 ms and then to various test potentials for 200 ms once every 2 s. *B*, τ, time constant of decay of the transient component of I_{Ca} is plotted as a function of test potential. *C*, the magnitude of the transient component of I_{Ca} is plotted as a function of test potential. The smooth curves are calculated using eqn (5), d_∞ and f_∞ from Fig. 3 and the following constants: neonatal $E_{channel} = +54$ mV, $g_r = 23{\cdot}38$ nS; adult $E_{channel} = +58$ mV, $g_r = 12{\cdot}11$ nS. *D*, current at the end of the 200 ms test pulse is plotted as a function of potential. Neonatal: □, control; +, Cd^{2+} (0·1 mM). Adult: ▼, control; ×, Cd^{2+} (0·1 mM).

To investigate f_∞ the membrane potential was held at −50 mV. Following a 200 ms voltage clamp step to V_{test}, the membrane potential was hyperpolarized to −90 mV for 10 ms, and then depolarized to the evaluation potential (+5 mV) for 200 ms before returning to the holding potential. To control for I_{Ca} 'run-down' all trials to V_{test} were alternated with trials to V_{test}^{max} (the test potential that gives the largest current transient at the evaluation potential) and the ratio of the resulting currents (I_{test}/I_{test}^{max}) is plotted in Fig. 3*C*. The smooth curve shows the best-fit line described by eqn (3) (neonatal constants: $V_h = 6{\cdot}8$ mV, $k = 9{\cdot}05$ mV; adult constants: $V_h = -21{\cdot}6$ mV, $k = 7{\cdot}15$ mV). f_∞ measured in adult cells is shifted in the hyperpolarizing direction by about 15 mV (shift in V_h) when compared to neonatal cells. Furthermore, f_∞ is steeper for the adult cells at 0 mV there is relatively little overlap of d_∞ and f_∞ (Fig. 3*D*) and there is little steady-state calcium current observed (Fig. 2*A* and *D*). Figure 3*E* shows a plot of the predicted shape of the

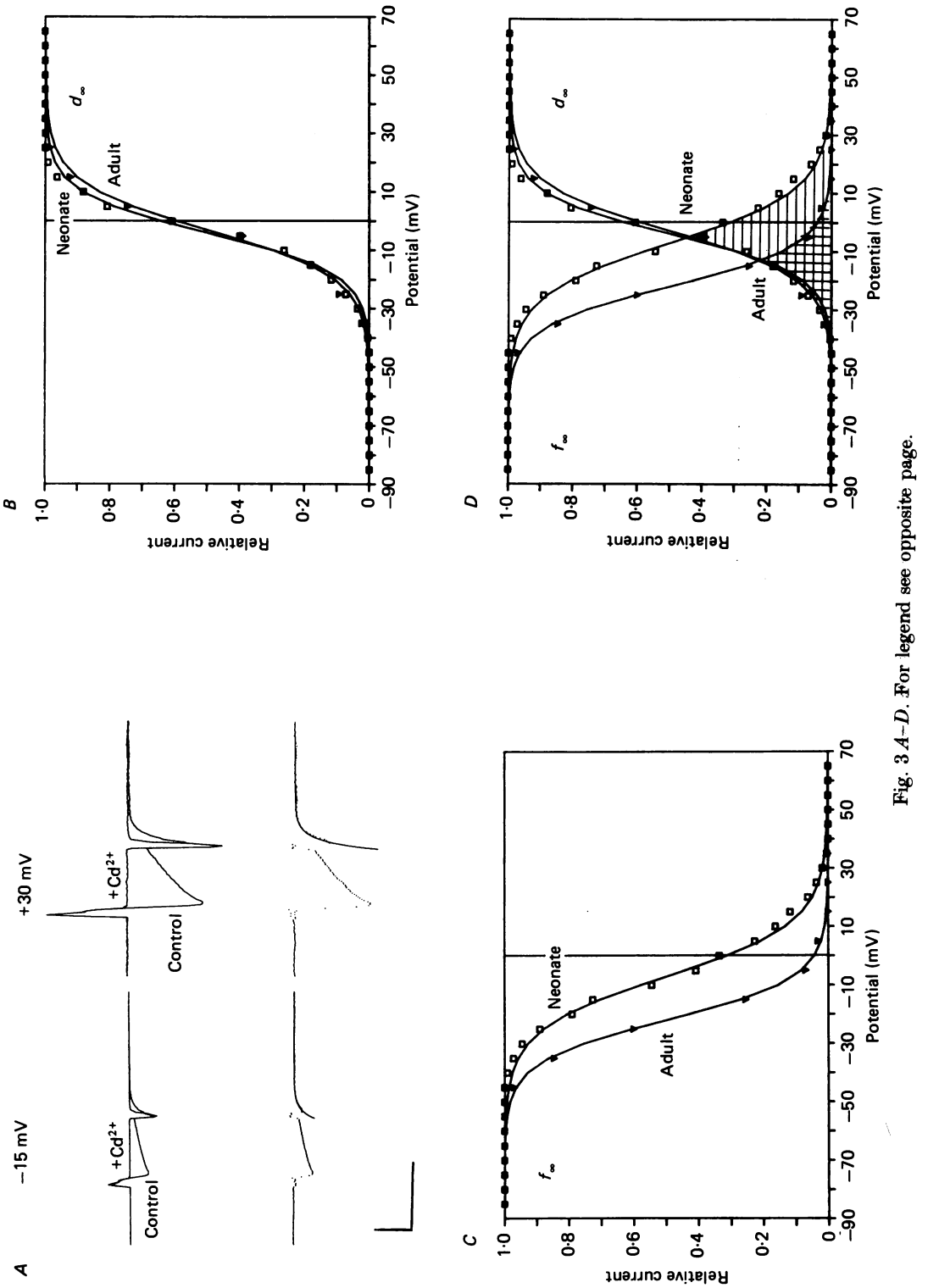

Fig. 3 *A–D*. For legend see opposite page.

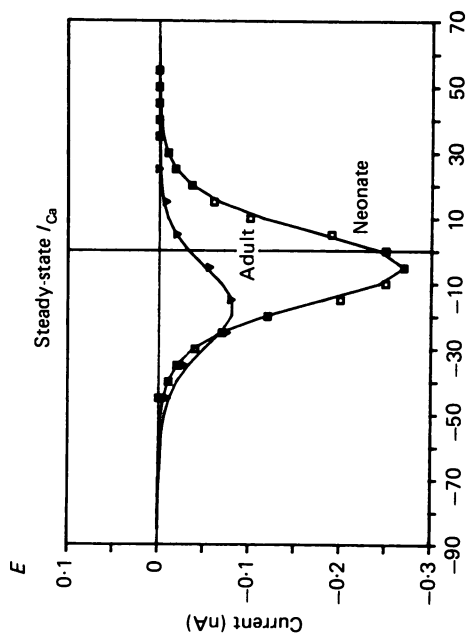

Fig. 3. Steady-state activation (d_∞) and inactivation (f_∞) variables in neonatal and adult heart cells. *A*, neonate original records used to measure steady-state activation. Tail currents were measured in the absence (control) and presence (+Cd^{2+}) of 0·1 mM-Cd^{2+} on return to the holding potential (−50 mV) from steps to different test potentials: $V_{test} = -15$ mV (left panel) and $V_{test} = +30$ mV (right panel). The lower traces represent I_{Ca}; the Cd^{2+}-subtracted records (points) and the monoexponential fits (continuous lines) as determined by the least-squares fitting process described in the Methods section. Time scale, 10 ms; current scale, 0·5 nA. *B*, steady-state activation (d_∞) is plotted as a function of potential. The tail current measured at the holding potential (−50 mV) following a test potential (I_{test}) is measured as is the maximum tail current (I_{test}^{max}). The ratio I_{test}/I_{test}^{max} is plotted as a function of V_{test}. The smooth curve is the best fit of the data to eqn (2) (see Methods). *C*, steady-state inactivation (f_∞) is plotted as a function of potential. The current elicited by a standard depolarization after stepping to a test potential for 200 ms and a 10 ms repolarization to −50 mV (I_{test}) is measured. The maximum current recorded using this procedure is also measured (I_{test}^{max}). The ratio I_{test}/I_{test}^{max} is plotted as a function of V_{test}. The smooth curve is the best fit of the data to eqn (3) (see Methods). *D*, overlap of d_∞ and f_∞. The curves showing the voltage dependence of d_∞ and f_∞ from panels *B* and *C* are plotted together. The overlap of d_∞ and f_∞ (hatched areas) represents, in each preparation, voltage ranges over which both d_∞ and f_∞ are non-zero and steady-state calcium current ('window current') will flow. *E*, the steady-state current–voltage relationship of I_{Ca}. Assuming that I_{Ca} 'relative conductance' (neonatal $g_r = 25{\cdot}72$ nS; adult $g_r = 22{\cdot}22$ nS) is not a function of voltage and that the reversal potential for I_{Ca} is $E_{channel}$ (neonatal $E_{channel} = +54$ mV; adult $E_{channel} = +58$ mV), the continuous lines are the calculated voltage dependence of the steady-state component of I_{Ca} from panel *D* and eqn (4). The data points represent the measured Cd^{2+}-sensitive steady-state I_{Ca}. The data values are calculated by subtracting the Cd^{2+}-blocked current (neonate, +; adult, ×) from the control current (neonate, □; adult, ▼) (recorded in the presence of 10 μM-TTX in the superfusion solution, and 20 mM-CsCl in the pipette solution) in Fig. 2*D*.

steady-state component of calcium current–voltage relationship (continuous lines) and the Cd^{2+}-sensitive steady-state current obtained from the results shown in Fig. 2*D* (points). The continuous line was calculated from the equation:

$$I_{Ca}^{\text{steady-state}}(V_m) = g_r \times (V_m - E_{\text{channel}}) \times d_\infty(V_m) \times f_\infty(V_m), \quad (4)$$

where g_r is a voltage-independent relative conductance variable (the only adjustable variable) and is adjusted to fit the data by eye. All other variables are measured experimentally. E_{channel} is the reversal potential of the current, and $d_\infty(V_m)$ and $f_\infty(V_m)$ are the appropriate d_∞ and f_∞ functions (Fig. 3). Note that the voltage dependence of the calculated steady-state I_{Ca} (continuous line) is similar to that of the Cd^{2+}-sensitive current (points).

The d_∞ and f_∞ functions can also be used to predict the transient I_{Ca}. In Fig. 2*C* the smooth curves were calculated from the equation:

$$I_{Ca}^{\text{transient}}(V_m) = g_r \times (V_m - E_{\text{channel}}) \times d_\infty(V_m) \times (1 - f_\infty(V_m)), \quad (5)$$

where g_r is a voltage-independent relative conductance variable (the only adjustable variable). All other variables are measured experimentally and include E_{channel} (the reversal potential of the current, Fig. 2*C*), and $d_\infty(V_m)$ and $f_\infty(V_m)$ (the appropriate d_∞ and f_∞ values, Fig. 3).

Modulation of the sarcoplasmic reticulum

Having observed clear differences between I_{Ca} in adult and neonatal rat cardiac myocytes, we sought to investigate what might be responsible. Differences in the sarcoplasmic reticulum in adult and neonatal heart cells (Hoerter *et al.* 1981; Fabiato, 1982; Nakanishi & Jarmakani, 1984; Seguchi, Harding & Jarmakani, 1986) and the availability of ryanodine, an agent that specifically interferes with sarcoplasmic reticulum function (Weber, 1968; Sutko, Willerson, Templeton, Jones & Besch, 1979; Sutko & Kenyon, 1983; Hess & Wier, 1984) led us to investigate the possible connection between the development of a functional sarcoplasmic reticulum and the changes in I_{Ca}.

The effects of ryanodine on adult myocytes

The effect of ryanodine on contraction. The plant alkaloid ryanodine is reported to exert a negative inotropic effect on both skeletal and cardiac muscle preparations (Jenden & Fairhurst, 1969). This effect is proposed to be a consequence of alterations in the function of the sarcoplasmic reticulum (Sutko *et al.* 1979). Specifically, at 'low' concentrations ($< 100\ \mu$M) it has been suggested to alter the action of a calcium-release channel in the sarcoplasmic reticulum (Meissner, 1986) with two ryanodine binding sites (Inui, Saito & Fleischer, 1987*a*) located on each tetrameric 'foot' (Ferguson, Schwartz & Franzini-Armstrong, 1984) connecting the sarcolemma or T-tubule to the sarcoplasmic reticulum (see Discussion). We have examined the effect of 10 μM-ryanodine on the twitch of adult rat single ventricular myocytes. The results are presented in Fig. 4. Depolarizing voltage clamp steps from the holding potential (−50 mV) to 0 mV for 200 ms were imposed at 0·5 Hz. Below the voltage trace are three sets of current and shortening records: control, 10 μM-ryanodine (3 min) and 10 μM-ryanodine (5 min). Cell shortening was measured using a video

dimension analyser (see Methods). On depolarization we observed both activation of an inward current (I_{Ca}) which inactivates rapidly to a maintained steady level, and cell shortening. Three minutes after adding 10 μM-ryanodine to the superfusion solution the transient component of I_{Ca} is larger, the steady-state inward current is

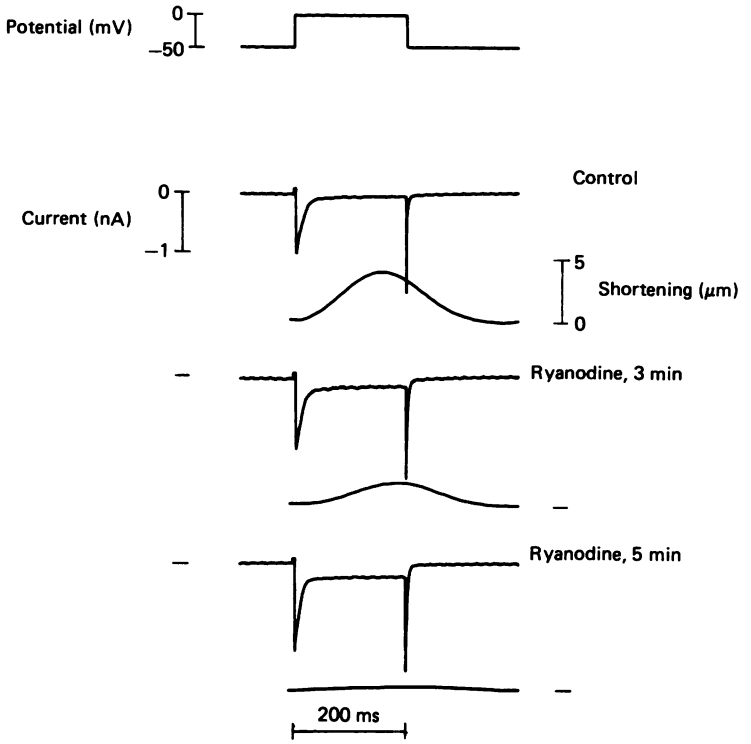

Fig. 4. The effect of ryanodine on I_{Ca} and contraction in single adult rat cardiac myocytes. A depolarizing voltage clamp step from the holding potential (−50 mV) to 0 mV for 200 ms elicited I_{Ca} and a contraction (measured as cell shortening). The three pairs of traces reflect I_{Ca} and the twitch under control conditions and 3 and 5 min after adding 10 μM-ryanodine to the superfusion solution.

larger, and the amount of cell shortening is decreased. Five minutes after addition of the ryanodine to the superfusion solution the transient component of I_{Ca} is increased still further, and the component of steady-state inward current is also further increased while cell shortening has been virtually abolished. This latter result on shortening is consistent with earlier investigation into the actions of ryanodine (Sutko *et al.* 1979; Mitchell *et al.* 1984; Bers, 1985).

The effects of ryanodine on adult I_{Ca}. Figure 5 shows how ryanodine alters I_{Ca} in adult rat heart. Figure 5*A* shows original records of I_{Ca} recorded in response to 200 ms depolarizing pulses to 0 mV from −50 mV applied at 0·5 Hz. In the presence of ryanodine (10 μM) there is an increase in both the transient and the steady-state components of I_{Ca}. Consistent with the increase in the steady-state component of I_{Ca}, is the increased inward tail current that is clearly visible on repolarization in the presence of ryanodine. Figure 5*B* shows that the voltage dependence of the

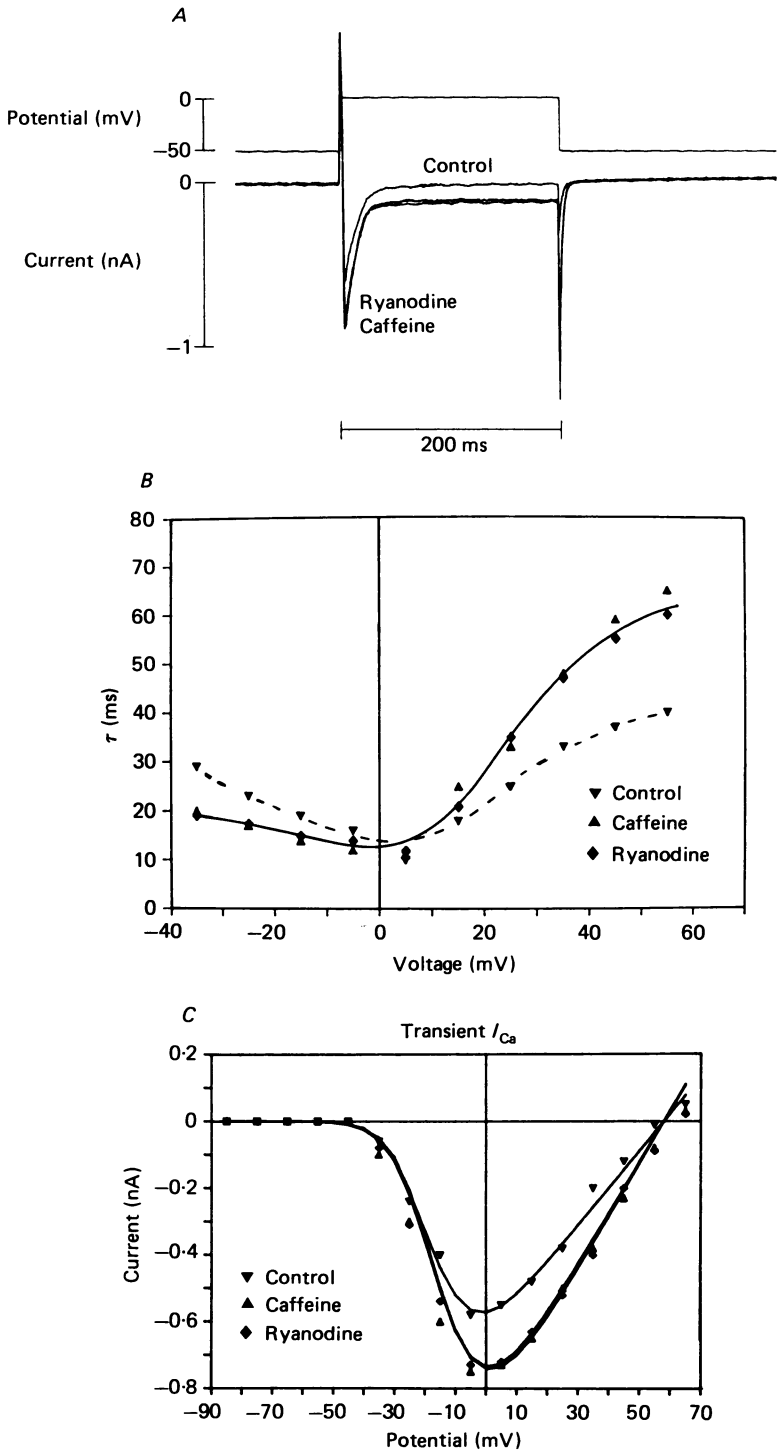

Fig. 5. For legend see facing page.

inactivation time constant is also altered by this agent. In untreated adult heart myocytes there is a 'U-shaped' curve (dashes). The time constant of inactivation (τ) is about 30 ms at −35 mV, decreasing to about 10 ms at 0 mV. Positive to 0 mV τ increases, reaching about 40 ms at +55 mV. Ryanodine makes the voltage dependence of the time constant of inactivation more sigmoid, decreasing τ at negative potentials while increasing it at positive potentials (continuous line). At −40 mV, τ is reduced by about one-third to 20 ms, remaining unchanged at 10 ms at 0 mV. At +55 mV the effect of ryanodine is to increase τ by 50% from 40 to about 60 ms. Ryanodine increases the magnitude of the transient component of I_{Ca} in adult ventricular myocytes without altering the voltage dependence of the transient component of I_{Ca} as is indicated in Fig. 5*C*. Figure 5 also shows that caffeine (10 mM) has actions similar to those of ryanodine.

The effect of ryanodine on adult d_∞ and f_∞. To further investigate the alteration of I_{Ca} in the adult cells when ryanodine is added we examined d_∞ and f_∞ using the same protocols described previously. Ryanodine did not have a significant effect on d_∞ as can be seen in Fig. 6*A*. However, ryanodine shifted f_∞ in the depolarizing direction (Fig. 6*B*) with a large positive shift in V_h and an increase in k (see Table 1). The effect of the alteration in f_∞ is shown in Fig. 6*C*. The blockade of sarcoplasmic reticulum function by ryanodine leads to an increase in the magnitude of the overlap of d_∞ and f_∞ with the overlap shifting to more positive potentials. These findings are consistent with the alterations in steady-state component of I_{Ca} observed in Fig. 5. From eqn (5), the relevant d_∞ and f_∞ functions (Fig. 6), the reversal potential of the current, $E_{channel}$ (Fig. 5*C*) and one free parameter (g_r) the voltage dependence of the transient component of I_{Ca} can be fitted as shown in Fig. 5*C*.

The results shown in Figs 5 and 6 raise the question whether the effects of ryanodine on f_∞ were due to a direct action of ryanodine on I_{Ca} inactivation or whether they may reflect an indirect effect of ryanodine which is mediated by intracellular Ca^{2+} ($[Ca^{2+}]_i$). To investigate this question the voltage clamp pipette solution was modified to decrease the magnitude of the $[Ca^{2+}]_i$ transient. We did this by adding a calcium buffer (either EGTA (10 or 20 mM) or BAPTA (10 mM)) to the pipette solution. The pipette solution for the EGTA experiments contained (in mM): caesium glutamate, 140; NaCl, 1; HEPES, 10; and K_2-EGTA/Ca-EGTA to yield a free $[Ca^{2+}]$ of about 100 nM and [EGTA] of 10 or 20 mM. On establishing a 'whole-cell' voltage clamp, depolarizing clamp steps from the holding potential (−50 mV) to 0 mV were imposed at 0·5 Hz to activate I_{Ca} and produce a twitch. A rapid reduction of the twitch was observed suggesting that the $[Ca^{2+}]_i$ transient within the cell was substantially reduced. (Fig. 7*A* and *B*). Figure 7*B* shows the original

---

Fig. 5. The steady-state effects of ryanodine and caffeine on adult I_{Ca}. *A*, original records of current and voltage. Currents were elicited by depolarizing steps for 200 ms to 0 mV from the holding potential (−50 mV) in the absence or the presence of either caffeine (10 mM) or ryanodine (10 μM). *B*, the effect of caffeine and ryanodine on the time constant of inactivation (τ) of I_{Ca}. *C*, the effect of caffeine and ryanodine on the transient component of I_{Ca}–voltage relationship. The smooth curves are predicted from the measured d_∞ and f_∞ (see Fig. 6) and eqn (5). ▼, control, g_r = 11·11 nS; ▲, caffeine (10 mM), g_r = 15·38 nS; ◆, ryanodine (10 μM), g_r = 15·87 nS. $E_{channel}$ = +58 mV.

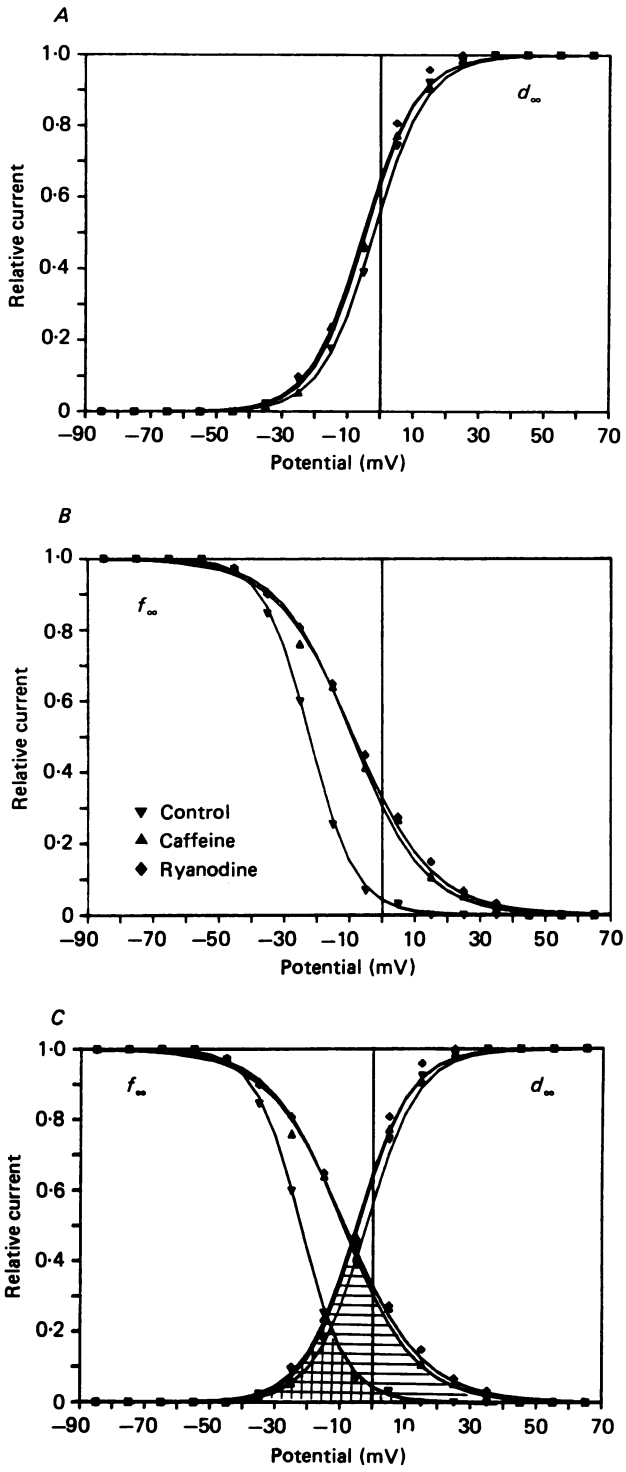

Fig. 6. For legend see facing page.

shortening records indicated by a,b,c, and d in Figure 7*A*. In the presence of 10 mM-EGTA, I_{Ca} magnitude is slightly increased and I_{Ca} inactivation is slightly slowed (Fig. 7*C*). After the twitch was abolished (record d) the voltage protocol described above to measure f_∞ was imposed and the results are displayed in Fig. 7*D*. Ryanodine (10 μM) was then added to the superfusion solution and 5 min later the voltage protocol to measure f_∞ was again imposed and the results are displayed in Fig. 7*E*. The effects of ryanodine under these 'buffered' conditions are very similar to those observed in the absence of buffer (and see Fig. 6*B*). This experiment was repeated in the presence of 20 mM-EGTA in the pipette and the effects on f_∞ were unchanged (Fig. 7*D* and *E*). This suggests that the effects of ryanodine on f_∞ may not depend to a great extent on changes in $[Ca^{2+}]_i$ since doubling the EGTA concentration in the pipette solution had no effect on the shift in f_∞ seen in the presence of ryanodine. If the effects of ryanodine do depend, in part, on $[Ca^{2+}]_i$, then the results suggest that there is an additional $[Ca^{2+}]_i$-independent mechanism.

A calcium buffer with faster kinetics was also used to cross-check the results seen with two concentrations of EGTA. BAPTA (Tsien, 1980) was added to the pipette solution so that it contained (in mM): caesium glutamate, 140; HEPES, 10; $CaCl_2$, 5; and BAPTA, 10. Although BAPTA more rapidly abolishes the twitch, its steady-state action to shift f_∞ (Fig. 7*D*) and slow τ (Fig. 7*C*) is similar to that of EGTA. Furthermore, the addition of ryanodine to BAPTA-buffered cells leads to a further shift in f_∞ as was seen with EGTA (Fig. 7*E*).

Figure 7*F* presents the results of pooled f_∞ data from all the experiments in which EGTA or BAPTA was included in the pipette solution. The data under three different conditions were fitted to eqn (3) using three different sets of constants: control (no ryanodine, no buffer) ($V_h = -21{\cdot}17$ mV, $k = 7{\cdot}14$ mV), buffered (without ryanodine) ($V_h = -17{\cdot}5$ mV, $k = 7{\cdot}67$ mV), and ryanodine (with or without buffer) ($V_h = -8{\cdot}0$ mV, $k = 10{\cdot}0$ mV) (see Table 1). A small and constant shift in f_∞ to more depolarized potentials was seen when free $[Ca^{2+}]$ was buffered to 100 nM and the $[Ca^{2+}]_i$ transient reduced regardless of the buffer (EGTA *vs.* BAPTA) or its concentration (10 mM-EGTA *vs.* 20 mM-EGTA). Moreover, the addition of ryanodine to the superfusion solution produced an equal shift in f_∞ whether or not the $[Ca^{2+}]_i$ transient was altered by the addition of an intracellular buffer. These experiments, therefore, suggest that although the ryanodine-dependent alteration of f_∞ might, in part, depend on $[Ca^{2+}]_i$, there is also a $[Ca^{2+}]_i$-independent mechanism.

The effects of ryanodine on neonatal myocytes

The effects of ryanodine on neonatal I_{Ca}. Figure 8 shows the effects of ryanodine on I_{Ca} in neonatal myocytes. Panel *A* presents records of I_{Ca} recorded in response to

---

Fig. 6. The effect of ryanodine and caffeine on the steady-state activation (d_∞) and inactivation (f_∞) variables of adult I_{Ca}. *A*, the effect of caffeine and ryanodine on steady-state activation (d_∞). ▼, control, $V_h = -1{\cdot}9$ mV, $k = 8$ mV; ▲, caffeine (10 mM), $V_h = -0{\cdot}5$ mV, $k = 8{\cdot}03$ mV; ◆, ryanodine (10 μM), $V_h = -0{\cdot}54$ mV, $k = 8{\cdot}18$ mV. *B*, the effect of caffeine and ryanodine on steady-state inactivation (f_∞). ▼, control, $V_h = -20{\cdot}7$ mV, $k = 7{\cdot}03$ mV; ▲, caffeine (10 mM), $V_h = -9{\cdot}1$ mV, $k = 8{\cdot}91$ mV; ◆, ryanodine (10 μM), $V_h = -8{\cdot}4$ mV, $k = 9{\cdot}11$ mV. *C*, the effect of caffeine and ryanodine on the overlap of d_∞ and f_∞.

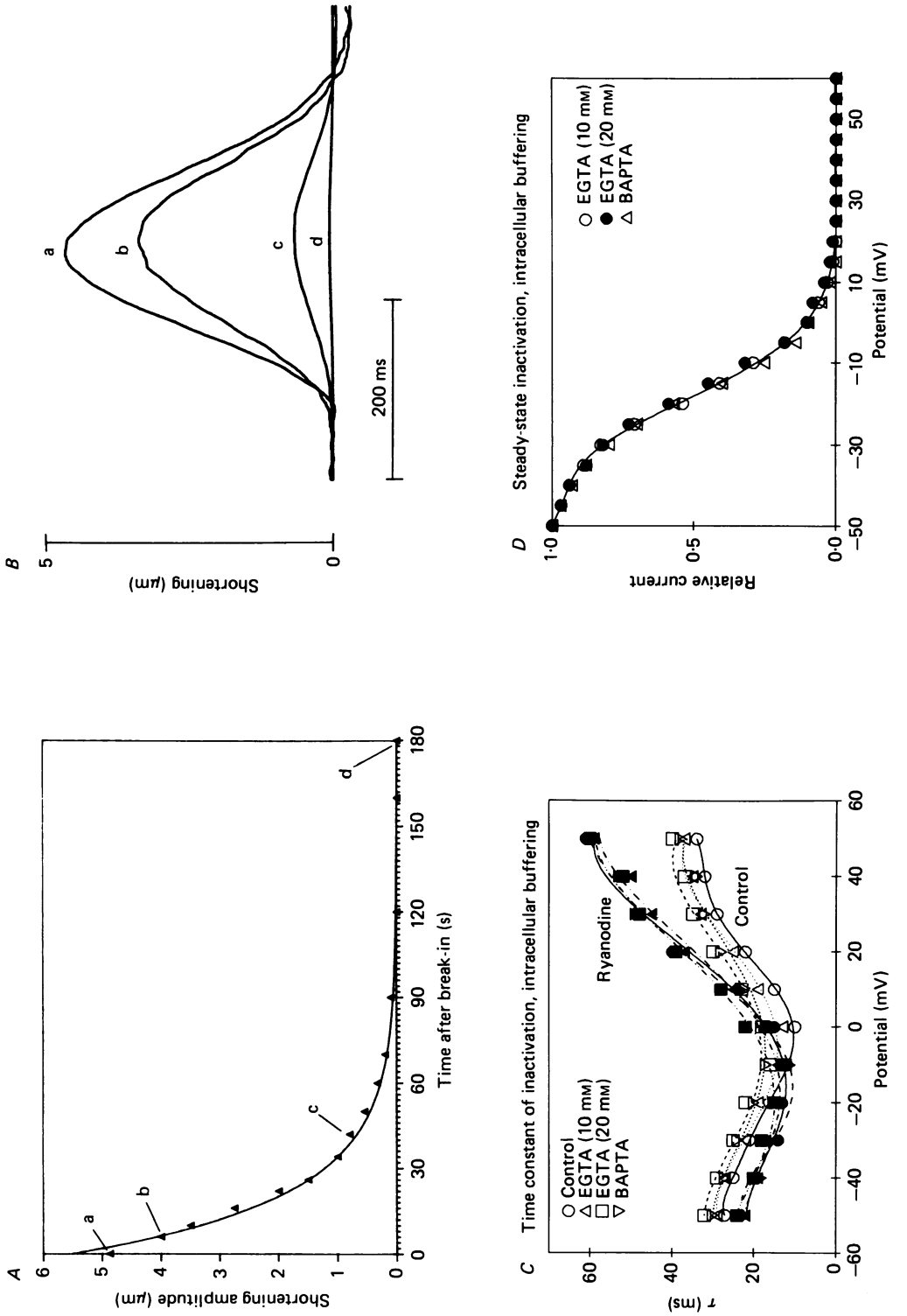

Fig. 7 *A–D*. For legend see facing page.

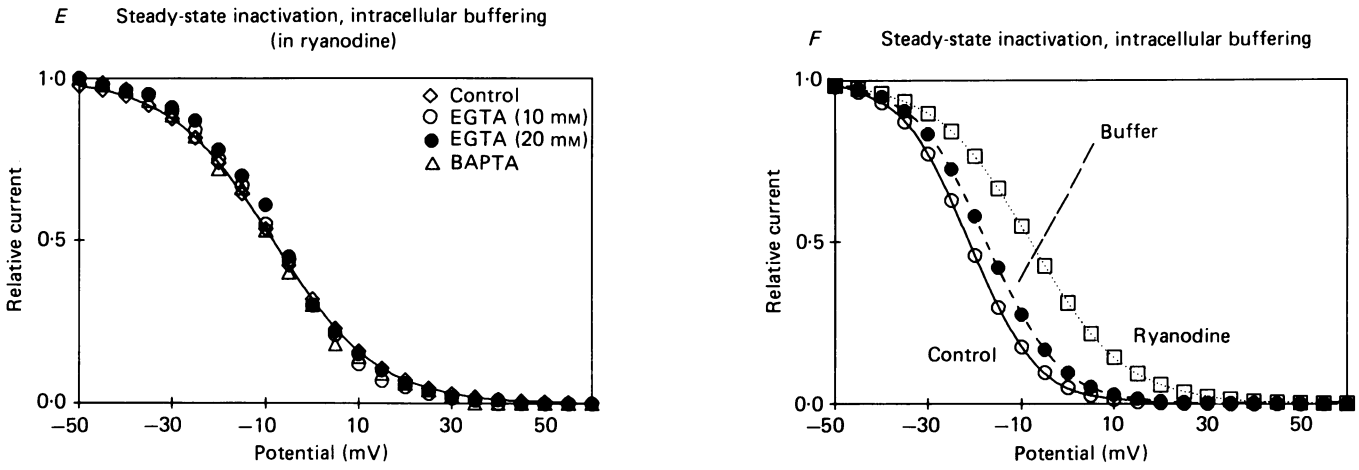

Fig. 7. The effect of intracellular calcium buffering on I_{Ca} and shortening. *A*, the time course of block of the twitch after establishing whole-cell voltage clamp with 10 mM-EGTA in the pipette. The twitch was elicited by a 200 ms depolarization to 0 mV from a holding potential of −50 mV. The time course of the decay of the twitch was fitted to a single-exponential equation by eye (*A* (estimated amplitude at time = 0 s) = 5·5 μm; τ = 20 s). *B*, shortening records were obtained at various times indicated in *A* and labelled a, b, c, and d. *C*, the effect of intracellular calcium buffering on the voltage dependence of the time constant of inactivation of the transient component of I_{Ca}. ○, control; △, 10 mM-EGTA; □, 20 mM-EGTA; ▽, BAPTA; ●, control + ryanodine; ▲, 10 mM-EGTA + ryanodine; ■, 20 mM-EGTA + ryanodine; ▼, BAPTA + ryanodine. Pipette-filling solutions as in panel *D*. *D*, f_∞ in the presence of 10 mM-EGTA (○), 20 mM-EGTA (●), or 10 mM-BAPTA (△) (see text). The continuous line is the fit of the pooled 'buffered' data to eqn (3) (V_h = −17·5 mV, k = 7·67 mV). *E*, f_∞ in the presence of 10 μM-ryanodine only (◇), 10 μM-ryanodine + 10 mM-EGTA (○), 10 μM-ryanodine + 20 mM-EGTA (●), or 10 μM-ryanodine + 10 mM-BAPTA (△). The continuous line is the fit of the pooled 'ryanodine' data to eqn (3) (V_h = −8 mV, k = 10 mV). *F*, f_∞ was measured in the absence (pooled 'control') and presence of EGTA or BAPTA (pooled 'buffered') and after the addition of ryanodine (10 μM) to the superfusion solution bathing the 'buffered' cells (pooled 'ryanodine'). Pooled data were fitted to eqn (3) using the following constants: 'control' (○), V_h = −21·17 mV, k = 7·14 mV; 'buffer' (●), V_h = −17·5 mV, k = 7·67 mV; 'ryanodine' (□), V_h = −8 mV, k = 10 mV. See Table 1 for statistics.

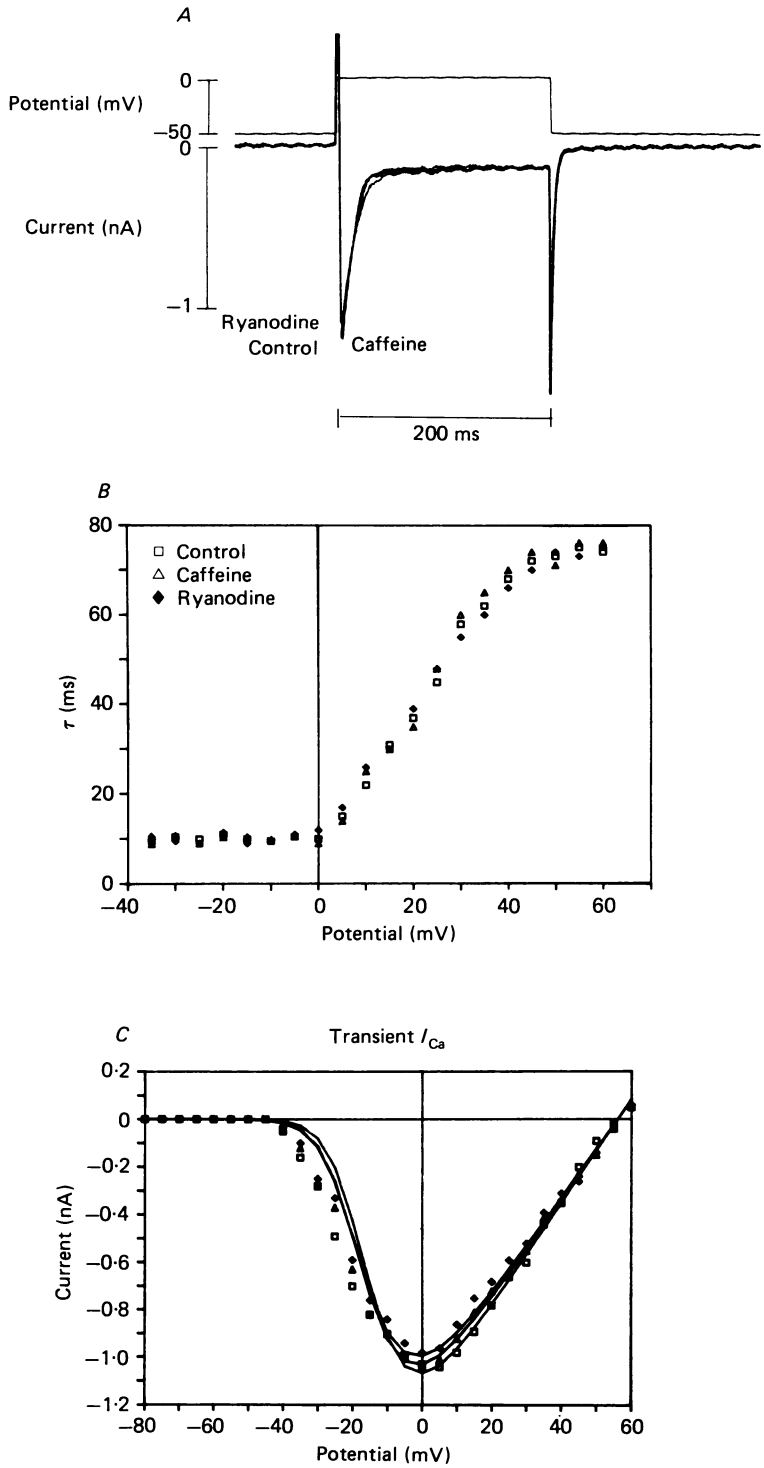

Fig. 8. For legend see facing page.

200 ms depolarizing pulses to 0 mV from −50 mV applied at 0·5 Hz under control conditions and after application of ryanodine. Under control conditions depolarization leads to a large inward current transient (transient component of I_{Ca}). The incomplete inactivation observed at the end of the 200 ms depolarizing step leads to a significant component of steady-state inward current (steady-state component of I_{Ca}). This is reflected by the inward tail current seen on repolarization. Ryanodine (10 μM) did not have any significant effect on these features of the neonatal I_{Ca}. Figure 8*B* shows that the voltage dependence of the inactivation time constant remains unchanged by ryanodine. This is a sigmoid-shaped curve with τ around 10 ms between −40 and 0 mV and increasing with greater depolarizations to about 75 ms at +55 mV. Figure 8*C* shows that the voltage dependence of the transient component of I_{Ca} is also little affected by ryanodine. Figure 8 also shows that caffeine (10 mM) similarly had no effects on the properties of I_{Ca}.

The effect of ryanodine on neonatal d_∞ and f_∞. The effect of ryanodine on d_∞ and f_∞ of neonatal I_{Ca} is shown in Figure 9. d_∞ is unchanged and f_∞ is only slightly altered. f_∞ was shifted in the hyperpolarizing direction with slight changes in both V_h and k (Table 1). With such minor changes in d_∞ and f_∞, the overlap of d_∞ and f_∞ remains essentially unchanged. This observation is consistent with the records of I_{Ca} in Fig. 8*A*. We have used eqn (5), the relevant d_∞ and f_∞ functions (Fig. 9), the reversal potential of the current, $E_{channel}$ (Fig. 8*C*) and a single adjustable factor (g_r) to fit the original data shown in Fig. 8*C*. Figure 9 also shows that caffeine and ryanodine had similar actions on d_∞ and f_∞.

The effect of EGTA and BAPTA on neonatal f_∞ and τ. Experiments were carried out on neonatal heart cells when either EGTA (10 mM) or BAPTA (10 mM) was included in the pipette solution. There was a slight shift of f_∞ to more depolarized potentials (see Table 1) but neither f_∞ or τ was found to be significantly different from control as shown in Fig. 10, given the number of experiments completed.

Ultrastructure parallel to effects of ryanodine

The significant differences in the effects of ryanodine on I_{Ca} in adult and neonatal heart cells suggest that reported differences between adult and neonatal preparations described in the literature (Penefsky, 1974; Hoerter *et al.* 1981; Page & Buecker, 1981; Maylie, 1982) were also present in adult single cells and the cultured neonatal cells used in our experiments.

Adult single myocytes. Plate 1*A* is an electron micrograph of a single adult rat myocyte at low magnification. This cell was prepared for electron microscopic examination after our usual enzymatic isolation procedure. A number of features are noteworthy. (1) The sarcolemmal (SL) edges are sharp and clear with no obvious

Fig. 8. The effect of caffeine and ryanodine on neonatal I_{Ca}. *A*, current was elicited by depolarizing steps for 200 ms to 0 mV from the holding potential (−50 mV) in the absence (control) or presence of either caffeine (10 mM) or ryanodine (10 μM). *B*, the effect of caffeine and ryanodine on the time constant of decay (τ) of I_{Ca}. *C*, the effect of caffeine and ryanodine on the transient component of I_{Ca}–voltage relationship. The smooth curves are predicted from the measured d_∞ and f_∞ (see Fig. 9) and eqn (5). □, control, g_r = 21·74 nS; △, caffeine (10 mM), g_r = 20·83 nS; ◆, ryanodine (10 μM), g_r = 20·41 nS. $E_{channel}$ = +56 mV.

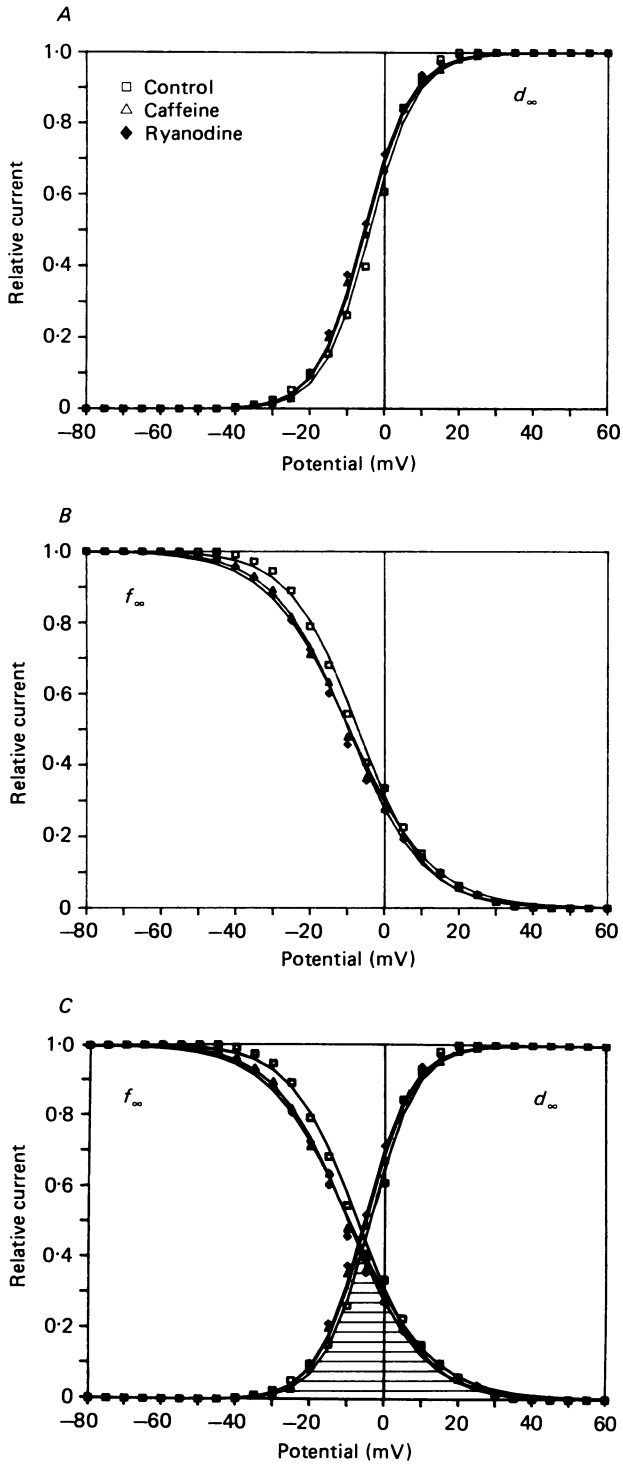

Fig. 9. For legend see facing page.

gross structural damage. (2) The cytoplasm is well organized with bands of myofilaments interspersed with mitochondria. The sarcomere structure is easily discernible. (3) There are invaginations of the sarcolemma along the Z-lines which may represent the sarcolemmal outlet of the T-tubule system. Plate 1 *B* is an electron micrograph of the same cell at higher magnification. There are organized myofilaments interspersed with mitochondria. The non-mitochondrial reticular structures at the Z-bands seen in association with the T-tubules constitute the sarcoplasmic reticulum.

Neonatal single myocytes. Plate 2 *A* is an electron micrograph at low magnification of a single neonatal rat myocyte obtained immediately after dissociation. There is a well-defined nucleus. In contrast to the adult cell, however, the cytoplasm of this cell is not highly organized. Sarcomeres are not readily visible although there are partially organized myofilaments and glycogen with groups of mitochondria. At higher magnification (Plate 2 *B*) the same cell shows the scarcity or absence of T-tubules (Hoerter *et al.* 1981) and no easily recognized sarcoplasmic reticulum.

DISCUSSION

We have examined I_{Ca} in neonatal and adult cardiac myocytes. There are differences in the relative magnitudes of the transient and steady-state components of I_{Ca} that can be described in terms of the steady-state activation and inactivation variables (d_∞ and f_∞), $E_{channel}$ (the reversal potential for I_{Ca}) and g_r (a relative conductance factor). When compared to neonatal heart cells, adult heart cells have reduced current density of I_{Ca}, a negative shift of f_∞, altered inactivation kinetics (faster at positive potentials, slower at negative potentials) and a reduction of the I_{Ca} 'window current' (see Cohen & Lederer, 1987 and Figs 2 and 3).

Sarcoplasmic reticulum during development

Neonatal heart cells have relatively little functional sarcoplasmic reticulum when compared to adult heart cells. Evidence supporting the relative absence of sarcoplasmic reticulum comes from many sources including contractile measurements (Seguchi *et al.* 1986), ultrastructural examinations (our Plate 1; Penefsky, 1974; Hoerter *et al.* 1981; Maylie, 1982), and biochemical studies (Naylor & Fassold, 1977; Fabiato & Fabiato, 1978; Bers *et al.* 1981; Nakanishi & Jarmakani, 1984). The sarcoplasmic reticulum may play little or no physiological role very early in development in many species (Penefsky, 1974; Fabiato & Fabiato, 1978; Bers *et al.* 1981; Boucek, Shelton, Artman & Landon, 1985). However, in adult cells, where the

---

Fig. 9. The effect of ryanodine and caffeine on steady-state activation (d_∞) and inactivation (f_∞) variables of neonatal I_{Ca}. *A*, the effect of ryanodine and caffeine on steady-state activation (d_∞). □, control, $V_h = -3{\cdot}5$ mV, $k = 6{\cdot}22$ mV; △, caffeine (10 mM), $V_h = -3{\cdot}9$ mV, $k = 6{\cdot}3$ mV; ◆, ryanodine (10 μM), $V_h = -4{\cdot}2$ mV, $k = 6{\cdot}24$ mV. *B*, the effect of caffeine and ryanodine on steady-state inactivation (f_∞). □, control, $V_h = -7{\cdot}03$ mV, $k = 9{\cdot}01$ mV; △, caffeine (10 mM), $V_h = -7{\cdot}6$ mV, $k = 8{\cdot}91$ mV; ◆, ryanodine (10 μM), $V_h = -7{\cdot}93$ mV, $k = 8{\cdot}87$ mV. *C*, the effect of caffeine and ryanodine on the overlap of d_∞ and f_∞.

TABLE 1. Parameters of I_{Ca}

			Control	Caffeine	Ryanodine	Buffered	Buffered + ryanodine
Adult	d_∞	V_h (mV)	$-1{\cdot}03 \pm 1{\cdot}7$	$-0{\cdot}68 \pm 1{\cdot}6$	$-0{\cdot}46 \pm 1{\cdot}5$	NA	NA
		k (mV)	$7{\cdot}95 \pm 0{\cdot}26$	$7{\cdot}92 \pm 0{\cdot}38$	$8{\cdot}12 \pm 0{\cdot}27$	NA	NA
	f_∞	V_h (mV)	$-21{\cdot}17 \pm 3{\cdot}4$	$-8{\cdot}4 \pm 1{\cdot}4$	$-8{\cdot}5 \pm 2{\cdot}4$	$-17{\cdot}5 \pm 2{\cdot}8$*	$-8{\cdot}0 \pm 2{\cdot}6$**
		k (mV)	$7{\cdot}14 \pm 0{\cdot}23$	$8{\cdot}78 \pm 0{\cdot}22$	$9{\cdot}08 \pm 0{\cdot}3$	$7{\cdot}67 \pm 0{\cdot}31$*	$10{\cdot}0 \pm 0{\cdot}29$**
	g_r	Transient (nS)	$12{\cdot}3 \pm 4$	$16{\cdot}1 \pm 5$	$15{\cdot}8 \pm 5$	NA	NA
		Steady-state (nS)	$12{\cdot}6 \pm 3$	NA	NA	NA	NA
	n	—	10	5	5	10	10
Neonate	d_∞	V_h (mV)	$-2{\cdot}96 \pm 1{\cdot}4$	$-3{\cdot}1 \pm 1{\cdot}4$	$-3{\cdot}5 \pm 1{\cdot}5$	NA	NA
		k (mV)	$6{\cdot}59 \pm 0{\cdot}67$	$6{\cdot}52 \pm 0{\cdot}3$	$6{\cdot}6 \pm 0{\cdot}34$	NA	NA
	f_∞	V_h (mV)	$-6{\cdot}93 \pm 2{\cdot}5$	$-7{\cdot}2 \pm 2{\cdot}5$	$-7{\cdot}38 \pm 2{\cdot}3$	$-5{\cdot}3$	$-6{\cdot}4$
		k (mV)	$9{\cdot}19 \pm 0{\cdot}6$	$9{\cdot}26 \pm 0{\cdot}56$	$9{\cdot}22 \pm 0{\cdot}4$	$9{\cdot}2$	$9{\cdot}5$
	g_r	Transient (nS)	$24{\cdot}9 \pm 5$	$22{\cdot}2 \pm 4$	$21{\cdot}8 \pm 4$	NA	NA
		Steady-state (nS)	$25{\cdot}2 \pm 3$	NA	NA	NA	NA
	n	—	10	5	5	3	3

* $P < 0{\cdot}05$ *vs.* control (two-tailed t test).
** $P < 0{\cdot}01$ *vs.* control and *vs.* buffered only (two-tailed t test).
NA, not applicable.

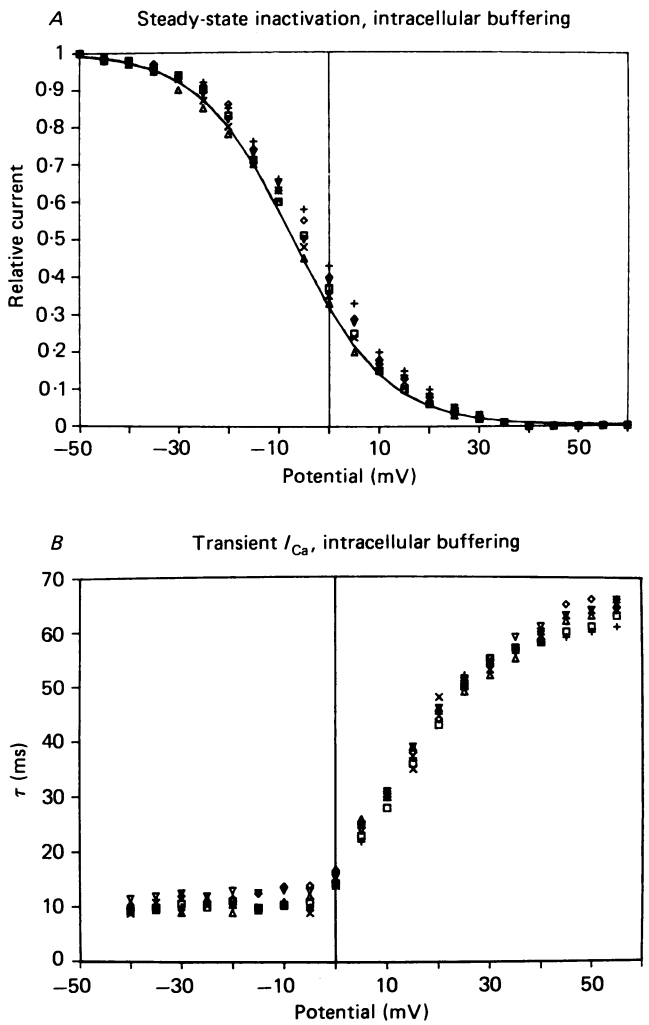

Fig. 10. The effect of increased intracellular calcium buffering and ryanodine on I_{Ca} in rat neonatal heart cells. *A*, we used our standard pipette solution with 140 mM-CsCl to which either EGTA and Ca^{2+} or BAPTA and Ca^{2+} were added to produce an estimated $[Ca^{2+}]_i$ of about 100 nM, pH = 7·38 and [EGTA] = 10 mM or [BAPTA] = 10 mM. f_∞ was measured in the absence (continuous line) and presence of EGTA (□, ×, ◇) or BAPTA (△, +, ▽). *B*, the effect of intracellular calcium buffering on the voltage dependence of the time constant of inactivation of the transient component of I_{Ca}. □, control; ◇, EGTA; ▽, BAPTA; +, control + ryanodine; △, EGTA + ryanodine; ×, BAPTA + ryanodine. Pipette-filling solutions as in panel *A*.

sarcoplasmic reticulum is a fundamental link in excitation–contraction coupling, alteration of sarcoplasmic reticulum function has a profound effect on contraction (cf. Fabiato, 1982; Bers, 1985). Thus, one of the aspects of postnatal development in the rat heart appears to be the organization of the contractile machinery into sarcomeres and the development of T-tubules and sarcoplasmic reticulum membranes.

I_{Ca} and the sarcoplasmic reticulum

An appealing explanation for the differences of I_{Ca} seen in the neonatal cells and in adult cells arises from the differences in anatomy of the two cell types. Adult cells, in contrast to neonatal cells, have a fully developed and functioning sarcoplasmic reticulum. A number of features of I_{Ca} normally seen in neonatal cells can be produced in adult cells pharmacologically by the application of ryanodine, a plant alkaloid that interferes with sarcoplasmic reticulum function. Similar effects are seen in the adult cells following the application of caffeine, another agent widely used to alter with sarcoplasmic reticulum function. However, neither ryanodine nor caffeine alters I_{Ca} (Fig. 8) in neonatal cells (which lack a fully functioning sarcoplasmic reticulum). We conclude from this latter point that neither ryanodine nor caffeine have a direct effect on the sarcolemmal calcium channel. Furthermore, from these experimental results, we conclude that interactions can occur between a functioning sarcoplasmic reticulum and I_{Ca}. Whatever the mechanism of interaction is, it appears to affect principally I_{Ca} inactivation.

Inactivation of I_{Ca}

Results of others. There is considerable evidence suggesting that Ca^{2+} may modulate I_{Ca} inactivation in heart (Mitchell, Powell, Terrar & Twist, 1983; Kass & Sanguinetti, 1984; Mentrard, Vassort & Fischmeister, 1984; Josephson, Sanchez-Chapula & Brown, 1984; Lee, Marban & Tsien, 1985). Two lines of evidence support this suggestion. The first kind of evidence links elevated $[Ca^{2+}]_i$ (measured by inference) with I_{Ca} inactivation. The 'double-pulse' experiment uses an initial ('conditioning') depolarization to activate I_{Ca} and thereby elevate $[Ca^{2+}]_i$. The effect of the initial depolarization is evaluated during the second ('test') pulse by measuring I_{Ca} (Mentrard *et al.* 1984; Josephson *et al.* 1984; Lee *et al.* 1985). These experiments have shown clear effects of the 'conditioning' pulse on the magnitude of I_{Ca} elicited by the 'test' depolarization. The second kind of evidence involves measuring I_{Ca} when a cation other than Ca^{2+} acts as the charge carrier. When Ba^{2+} (Mitchell *et al.* 1983; Josephson *et al.* 1984; Kass & Sanguinetti, 1984; Lee *et al.* 1985), Sr^{2+} (Mitchell *et al.* 1983; Kass & Sanguinetti, 1984; Lee *et al.* 1985), or Na^{+} (Hess & Tsien, 1984; Hess, Lansman & Tsien, 1986; Hadley & Hume, 1987) is used to carry current in place of Ca^{2+}, inactivation is significantly reduced. The conclusion reached from these experiments is that calcium plays an important role in the inactivation of I_{Ca} but that other (voltage-dependent) processes are also involved. The site at which the Ca^{2+} acts to influence inactivation has not yet been determined. Our data, however, suggest that the site at which Ca^{2+} influences I_{Ca} inactivation may be largely within the channel pore (see below).

Neonate vs. adult. Can $[Ca^{2+}]_i$-dependent inactivation account for the differences in I_{Ca} seen in neonatal and adult cells? The presence of a functional sarcoplasmic reticulum in adult cells could lead to higher $[Ca^{2+}]_i$ on depolarization. This could lead to altered kinetics of inactivation in the adult *vs.* the neonatal heart cells if $[Ca^{2+}]_i$-dependent inactivation plays a large role. The more rapid inactivation of I_{Ca} in adult cells at potentials positive to 0 mV (Fig. 2*B*), the leftward shift of f_∞ (Fig. 3) in the adult and the removal of these differences by ryanodine (Figs 5*B* and 6) are consistent with this hypothesis.

To examine whether the actions of ryanodine on I_{Ca} kinetics could be mediated by altered sarcoplasmic reticulum calcium release, $[Ca^{2+}]_i$ was buffered with intracellular EGTA or BAPTA (Fig. 7). We observed that the twitch in the adult cells was abolished by the application of either intracellular EGTA or BAPTA suggesting that the spatially averaged $[Ca^{2+}]_i$ during the depolarization does not rise as it usually does. The inactivation rate of I_{Ca} was slowed and the f_∞ curve was shifted to the right by a small amount by the intracellular EGTA or BAPTA (consistent with earlier reports of Josephson *et al.* 1984). However, subsequent application of ryanodine led to large additional changes in both f_∞ and τ, with the final shift being similar to that seen in the absence of EGTA or BAPTA but with ryanodine alone (Fig. 7). These experiments suggest that a part of the difference in adult and neonatal I_{Ca} may be due to $[Ca^{2+}]_i$-dependent alterations in I_{Ca} kinetics. The novel finding, however, is that ryanodine appears to have additional actions on I_{Ca} kinetics in adult myocytes which appear to be independent of the effects of ryanodine on $[Ca^{2+}]_i$. An alternative explanation that cannot be excluded is that both 10 and 20 mM-EGTA or 10 mM-BAPTA cannot adequately control $[Ca^{2+}]_i$ at a specific intracellular site where Ca^{2+} acts to modify I_{Ca}. Barring this explanation, which we cannot readily test further, we tentatively conclude that ryanodine can act to alter I_{Ca} by some means that is not mediated by $[Ca^{2+}]_i$. Since ryanodine has no effect on neonatal I_{Ca} (Figs 8 and 9), we conclude that when ryanodine affects I_{Ca} in adult cells, it, too, does not act on the sarcolemmal calcium channel directly.

What causes the shift in f_∞? The simplest explanation for the $[Ca^{2+}]_i$-independent action of ryanodine involves ryanodine binding to the spanning protein (or 'feet') linking the sarcolemma to the sarcoplasmic reticulum. Inui *et al.* (1987*a*, *b*), Lai, Erickson, Block & Meissner (1987) and Hymel, Inui, Fleischer & Schindler (1988) have presented evidence that the ryanodine binding site in both skeletal muscle and cardiac muscle is on the feet protein. Other recent reports have suggested that this spanning protein can be found even on purified sarcoplasmic reticulum vesicles, has four subunits (Ferguson *et al.* 1984), and two binding sites for ryanodine (Inui *et al.* 1987*a*). Inasmuch as the spanning protein remains with the isolated vesicles, the same ryanodine binding site that affects sarcoplasmic reticulum calcium release in intact cells may account for the modulation of sarcoplasmic reticulum calcium-release channels incorporated into artificial bilayers (from the vesicle preparation) as well (Imagawa, Smith, Coronado & Campbell, 1987). Since ryanodine binds to a site on the spanning protein (Inui *et al.* 1987*a*, *b*) and thereby affects the sarcoplasmic reticulum calcium-release channel (Imagawa *et al.* 1987; Hymel *et al.* 1987), ryanodine's binding to the feet structures could, in principle, also affect the sarcolemmal calcium channel as we suggest below.

Model

Links between the sarcolemma and the sarcoplasmic reticulum. Recent experimental results in skeletal muscle have linked the binding of a dihydropyridine (DHP) calcium channel blocker to reduced intramembrane charge movement as well as reduced calcium release from the sarcoplasmic reticulum (Rios & Brum, 1987). Although the authors suggest that the binding site in skeletal muscle for dihydropyridines probably does not involve a functional calcium channel, the protein involved may resemble a calcium channel or be a 'vestigial' or 'dormant'

calcium channel (see Schwartz, McCleskey & Almers, 1985). Regardless of the exact identity of the dihydropyridine receptor, these results show that a sarcolemmal receptor is linked to the sarcoplasmic reticulum calcium-release channel. These results, combined with those suggesting that the spanning protein and the sarcoplasmic reticulum calcium-release channel are related (Imagawa *et al.* 1987; Inui *et al.* 1987*a*, *b*; Hymel *et al.* 1987), suggest that the spanning protein serves as a mechanical link between the sarcolemma and the sarcoplasmic reticulum. This interpretation is also suggested by our results as indicated below.

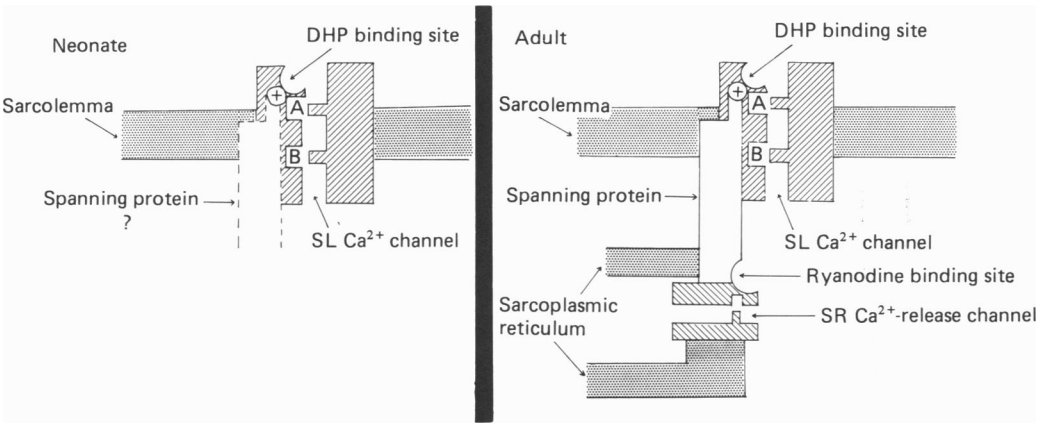

Fig. 11. Model of excitation–contraction mechanisms in neonatal and adult heart cells. In the neonatal cells (left), where a functional sarcoplasmic reticulum appears to be absent, the rise of $[Ca^{2+}]_i$ during the $[Ca^{2+}]_i$ transient depends on transarcolemmal flux. In the adult cells (right), the sarcoplasmic reticulum also releases calcium, thereby augmenting the $[Ca^{2+}]_i$ transient seen on depolarization. The assigned roles of various elements in this model are given in Table 2 and in the text.

A principal difference between skeletal muscle and heart muscle is the larger number of functional calcium channels in heart muscle. We have made use of this important difference between heart and skeletal muscle, the biochemical identification of the spanning protein and calcium-release channel in the two tissues, and our own new results to suggest the mechanism for excitation–contraction coupling illustrated in Fig. 11. We have assumed that in our rat heart cells a *functional* calcium channel could substitute for the dihydropyridine binding site of Rios & Brum (1987). Furthermore, we have assumed that the '$[Ca^{2+}]_i$-independent' action of ryanodine on I_{Ca} requires ryanodine to bind to its receptor(s) on the spanning protein (Inui *et al.* 1987*a*, *b*; see also Sutko & Kenyon, 1983; Lundblad, Gonzalez-Seratos, Inesi, Swanson & Paolini, 1986). In neonatal cells (Fig. 11, left panel), where there is little functional sarcoplasmic reticulum, the principal source of Ca^{2+} for the activation of contraction is the transarcolemmal flux (e.g. I_{Ca}, Na^+–Ca^{2+} exchange, etc.). However, in the adult cells (Fig. 11, right panel), where a functional sarcoplasmic reticulum is linked to the surface membrane via the spanning protein, depolarization results in the opening of both surface membrane calcium channels (I_{Ca}) as well as the sarcoplasmic reticulum calcium-release channels.

There are three elements in our explanation each of which has been described in the literature.

TABLE 2. Model: possible proteins in excitation–contraction coupling

	SL Ca^{2+} channel protein(s)	Spanning protein(s)	SR Ca^{2+}-release channel protein(s)
Neonate	+	Unknown	Unknown
Adult	+	+	+
Ryanodine binding site	–	+/–	+/–
DHP binding site	+	–	–
Notes:	(i) Ca^{2+}-dependent inactivation (intrachannel site *vs.* site on intra-cellular domain of protein). (ii) May be influenced by SR Ca^{2+} release channel, $[Ca^{2+}]_i$, and ryanodine.	(i) Function labile. (ii) Independent link between SL Ca^{2+} channel and SR Ca^{2+} channel. (iii) Anatomical feature. (iv) Biochemical evidence. (v) Links intramembrane charge movements, DHP binding site, and ryanodine binding site.	(i) Positioned by spanning protein. (ii) Release may also be activated by $[Ca^{2+}]_i$.

The sarcolemmal (SL) calcium channel protein. This protein may have two binding sites for Ca^{2+}, A and B (Hess & Tsien, 1984; Hess *et al.* 1986; Lansman, Hess & Tsien, 1986, but see Yue & Marban, 1987) as Ca^{2+} permeates the pore in a single file. The binding of a dihydropyridine calcium channel blocker to the channel protein can both block Ca^{2+} permeation and also, we speculate, immobilize intramembrane charge movement associated with excitation–contraction coupling. The region of the sarcolemmal calcium channel protein that controls the Ca^{2+}-dependent inactivation of I_{Ca} may reside largely within the channel (and could even involve site A or B). This suggestion stems from the remarkably small influence of EGTA and BAPTA on both f_∞ and τ and the large action of alternative charge carriers (e.g. Na^+, Ba^{2+}, or Sr^{2+}) on I_{Ca} inactivation. A possible explanation of how EGTA and BAPTA may influence inactivation of I_{Ca} in adult heart involves their action on $[Ca^{2+}]_i$ near the sarcoplasmic reticulum calcium-release channel and the influence $[Ca^{2+}]_i$ may impose on the sarcoplasmic reticulum and the spanning protein(s) (see below).

The spanning protein. The spanning protein or 'foot process' serves as a physical anchor to position the sarcoplasmic reticulum near the sarcolemmal or T-tubular calcium channel. Additionally, it seems likely that the spanning protein acts to transmit information both ways between the sarcoplasmic reticulum and the sarcolemma (or T-tubule). The spanning protein serves to link the calcium channel in the sarcolemma (containing the sarcolemmal sensor responsible for intramembrane charge movement, as well as the dihydropyridine binding site) with the ryanodine binding site and the sarcoplasmic reticulum calcium-release channel. Furthermore, the action of modulators of this system (e.g. $[Ca^{2+}]_i$) may be transmitted to both the sarcoplasmic reticulum calcium-release channel and the sarcolemmal calcium channel via the spanning protein.

The sarcoplasmic reticulum (SR) calcium-release channel. This channel is positioned near the sarcolemmal calcium channel by the spanning protein. Its calcium-release function may be influenced both by the voltage across the sarcolemma, by $[Ca^{2+}]_i$, as well as by agents like ryanodine. At least some of these agents can act on the calcium-release channel by means of the spanning protein. Recent evidence suggests that the sarcoplasmic reticulum calcium-release channel and the spanning protein may be specialized domains of a single large (460 kD) protein.

The 'new' element in this model is the *two-way communication link* involving the spanning protein. A number of the features of the model have been previously described by others for cardiac and skeletal muscle (Schneider & Chandler, 1973; Chandler, Rokowski & Schneider, 1976*a*,*b*; Page & Bucker, 1981; Pessah, Waterhouse & Casida, 1985; Pessah, Francini, Scales, Waterhouse & Casida, 1986; Rios & Brum, 1987; Inui *et al.* 1987*a*,*b*; Imagawa *et al.* 1987; Lai *et al.* 1987; Hymel *et al.* 1988). Ryanodine binding to the spanning protein (or the sarcoplasmic reticulum calcium-release channel) can affect the sarcolemmal calcium channel in this model, and presumably appropriate antagonist binding to the sarcolemmal calcium channel can influence the sarcoplasmic reticulum calcium-release channel. The model can therefore readily explain how (1) changes in surface membrane potential affect sarcoplasmic reticulum calcium release, (2) sarcolemmal calcium channels 'directly' influence sarcoplasmic reticulum calcium-release channels, (3)

sarcoplasmic reticulum calcium-release channels 'directly' influence sarcolemmal calcium channels, and (4) Ca^{2+}-dependent modulation of both sarcoplasmic reticulum calcium-release channels and sarcolemmal calcium channels come about.

This work has been supported by the National Institutes of Health (HL 25675 and HL 36074) and the American and Maryland Heart Associations. The work was carried out during the tenure of an Established Investigator award supported by the American and Maryland Heart Associations (W.J.L.). We are indebted to Dr W. J. Mergner and S. Tepper for assistance in preparing the electron micrographs, Drs J. R. Berlin, M. B. Cannell, C. G. Nichols and G. L. Smith for valuable discussion and to Dr T. B. Rogers for loan of the video edge tracking equipment. We would like to thank Ms K. E. MacEachern for technical assistance. N.M.C. is grateful for the support of the Pharmaceutical Manufacturers Association Foundation.

REFERENCES

BEAN, B. P. (1984). Nitrendipine block of cardiac calcium channels: high affinity binding to the inactivated state. *Proceedings of the National Academy of Sciences of the U.S.A.* **81**, 6388–6392.

BERS, D. M. (1985). Ca influx and sarcoplasmic reticulum Ca release in cardiac muscle activation during postrest recovery. *American Journal of Physiology* **248**, H366–381.

BERS, D. M., PHILIPSON, K. D. & LANGER, G. A. (1981). Cardiac contractility and sarcolemmal calcium binding in several cardiac muscle preparations. *American Journal of Physiology* **240**, H576–583.

BEZANILLA, F. (1985). A high capacity data recording device based on a digital audio processor and a video cassette recorder. *Biophysical Journal* **47**, 437–441.

BOUCEK JR, R. J., SHELTON, M. E., ARTMAN, M. & LANDON, E. (1985). Myocellular calcium regulation by the sarcolemmal membrane in the adult and immature rabbit heart. *Basic Research in Cardiology* **80**, 316–325.

BOUCEK JR, R. J., SHELTON, M., ARTMAN, M., MUSHLIN, P. S., STARNES, V. & OLSON, R. D. (1984). Comparative effects of verapamil, nifedipine, and diltiazem on contractile function in the isolated immature and adult rabbit heart. *Pediatric Research* **18**, 948–952.

BYERLY, L. & HAGIWARA, S. (1982). Calcium currents in internally perfused nerve cell bodies of *Limnea stagnalis*. *Journal of Physiology* **322**, 503–528.

CHANDLER, W. K., ROKOWSKI, R. F. & SCHNEIDER, M. F. (1976*a*). A non-linear voltage dependent charge movement in frog skeletal muscle. *Journal of Physiology* **254**, 245–283.

CHANDLER, W. K., ROKOWSKI, R. F. & SCHNEIDER, M. F. (1976*b*). Effects of glycerol treatment and maintained depolarization on charge movement in skeletal muscle. *Journal of Physiology* **254**, 285–316.

COHEN, N. M. & LEDERER, W. J. (1986). Developmental changes in the steady-state kinetic parameters of the calcium current in isolated rat heart cells. *Journal of General Physiology* **88**, 17a.

COHEN, N. M. & LEDERER, W. J. (1987). Calcium current in isolated neonatal rat ventricular myocytes. *Journal of Physiology* **391**, 169–191.

FABIATO, A. (1982). Calcium release in skinned cardiac cells: variations with species, tissues, and development. *Federation Proceedings* **41**, 2238–2244.

FABIATO, A. & FABIATO, F. (1978). Calcium-induced release of calcium from the sarcoplasmic reticulum of skinned cells from adult human, dog, cat, rabbit, rat, and frog hearts and from fetal and new-born rat ventricles. *Annals of the New York Academy of Sciences* **307**, 491–522.

FENWICK, E. M., MARTY, A. & NEHER, E. (1982). Sodium and calcium channels in bovine chromaffin cells. *Journal of Physiology* **311**, 599–635.

FERGUSON, D. G., SCHWARTZ, H. W. & FRANZINI-ARMSTRONG, C. (1984). Subunit structure of junctional feet in triads of skeletal muscle: a freeze-drying, rotary-shadowing study. *Journal of Cell Biology* **99**, 1735–1742.

HADLEY, R. W. & HUME, J. R. (1987). An intrinsic potential-dependent inactivation mechanism associated with calcium channels in guinea-pig myocytes. *Journal of Physiology* **389**, 205–222.

HAMILL, O. P., MARTY, A., NEHER, E., SAKMANN, B. & SIGWORTH, F. J. (1981). Improved patch-

clamp techniques for high resolution current recording from cells and cell-free membrane patches. *Pflügers Archiv* **391**, 85–100.

HESS, P., LANSMAN, J. B. & TSIEN, R. W. (1986). Calcium channel selectivity for divalent and monovalent cations. Voltage and concentration dependence of single channel current in ventricular heart cells. *Journal of General Physiology* **88**, 293–319.

HESS, P. & TSIEN, R. W. (1984). Mechanism of ion permeation through calcium channels. *Nature* **309**, 453–456.

HESS, P. & WIER, W. G. (1984). Excitation–contraction coupling in cardiac Purkinje fibers. Effects of caffeine on the intracellular [Ca^{2+}] transient, membrane currents, and contraction. *Journal of General Physiology* **83**, 417–433.

HIRAKOW, R. & GOTOH, T. (1975). A quantitative ultrastructural study on the developing rat heart. In *Developmental and Physiological Correlates of Cardiac Muscle*, ed. LIEBERMAN, M. & SANO, T., pp. 37–49. New York: Raven Press.

HOERTER, J., MAZET, F. & VASSORT, G. (1981). Perinatal growth of the rabbit cardiac cell: possible implications for the mechanism of relaxation. *Journal of Molecular and Cellular Cardiology* **13**, 725–740.

HYMEL, L., INUI, M., FLEISCHER, S. & SCHINDLER, H. (1988). Purified ryanodine receptor of skeletal muscle sarcoplasmic reticulum forms Ca^{2+}-activated oligomeric Ca^{2+} channels in planar bilayers. *Proceedings of the National Academy of Sciences of the U.S.A.* **85**, 441–445.

IMAGAWA, T., SMITH, J. S., CORONADO, R. & CAMPBELL, K. P. (1987). Purified ryanodine receptor from skeletal muscle sarcoplasmic reticulum is the Ca^{2+}-permeable pore of the calcium release channel. *Journal of Biological Chemistry* **262**(34), 16636–16643.

INUI, M., SAITO, A. & FLEISCHER, S. (1987*a*). Purification of the ryanodine receptor and identity with feet structures of junctional terminal cisternae of sarcoplasmic reticulum from fast skeletal muscle. *Journal of Biological Chemistry* **262**, 1740–1747.

INUI, M., SAITO, A. & FLEISCHER, S. (1987*b*). Isolation of the ryanodine receptor from cardiac sarcoplasmic reticulum and identity with the feet structures. *Journal of Biological Chemistry* **262**, 15637–15642.

ISENBERG, G. & KLOCKNER, U. (1982). Calcium currents of isolated bovine ventricular myocytes are fast and of large amplitude. *Pflügers Archiv* **395**, 30–41.

ISHIKAWA, H. & YAMADA, E. (1975). Differentiation of the sarcoplasmic reticulum and T-system in developing mouse cardiac muscle. In *Developmental and Physiological Correlates of Cardiac Muscle*, ed. LIEBERMAN, M. & SANO, T., pp. 21–35. New York: Raven Press.

JENDEN, D. J. & FAIRHURST, A. S. (1969). The pharmacology of ryanodine. *Pharmacological Reviews* **21**, 1–25.

JOSEPHSON, I. R., SANCHEZ-CHAPULA, J. & BROWN, A. M. (1984). A comparison of calcium currents in rat and guinea pig single ventricular cells. *Circulation Research* **54**, 144–156.

KASS, R. S. & SANGUINETTI, M. C. (1984). Inactivation of calcium channel current in the calf cardiac Purkinje fiber. Evidence for voltage- and calcium-mediated mechanisms. *Journal of General Physiology* **84**, 705–726.

LAI, F. A., ERICKSON, H., BLOCK, B. A. & MEISSNER, G. (1987). Evidence for junctional feet–ryanodine receptor complex from sarcoplasmic reticulum. *Biochemical and Biophysical Research Communications* **143**, 704–709.

LANGER, G. A., BRADY, A. J., TAN, S. T. & SERENA, S. D. (1975). Correlation of the glycoside response, the force staircase, and the action potential configuration in the neonatal rat heart. *Circulation Research* **36**, 744–752.

LANSMAN, J. B., HESS, P. & TSIEN, R. W. (1986). Blockade of current through single calcium channels by Cd^{2+}, Mg^{2+}, and Ca^{2+}. Voltage and concentration dependence of calcium entry into the pore. *Journal of General Physiology* **88**, 321–347.

LEE, K. S., MARBAN, E. & TSIEN, R. W. (1985). Inactivation of calcium channels in mammalian heart cells: joint dependence on membrane potential and intracellular calcium. *Journal of Physiology* **364**, 395–411.

LEE, K. S. & TSIEN, R. W. (1982). Reversal of current through calcium channels in dialyzed single heart cells. *Nature* **297**, 498–501.

LEE, K. S. & TSIEN, R. W. (1984). High selectivity of calcium channels in single dialysed heart cells of the guinea-pig. *Journal of Physiology* **354**, 253–272.

LEGATO, M. J. (1975). Ultrastructural changes during normal growth in dog and rat ventricular myofiber. In *Developmental and Physiological Correlates of Cardiac Muscle*, ed. LIEBERMAN, M. & SANO, T., pp. 249–274. New York: Raven Press.

LUNDBLAD, A., GONZALEZ-SERATOS, H., INESI, G., SWANSON, J. & PAOLINI, P. (1986). Patterns of sarcomere activation, temperature dependence, and effect of ryanodine in chemically skinned cardiac fibers. *Journal of General Physiology* **87**, 885–905.

MCDOWELL, E. M. & TRUMP, B. F. (1976). Histologic fixatives suitable for diagnostic light and electron microscopy. *Archives of Pathology and Laboratory Medicine* **100**, 405–414.

MAYLIE, J. G. (1982). Excitation–contraction coupling in neonatal and adult myocardium of cat. *American Journal of Physiology* **242**, H834–843.

MEISSNER, G. (1986). Ryanodine activation and inactivation of the Ca^{2+} release channel of sarcoplasmic reticulum. *Journal of Biological Chemistry* **261**, 6300–6306.

MENTRARD, D., VASSORT, G. & FISCHMEISTER, R. (1984). Calcium-mediated inactivation of the calcium conductance in cesium-loaded frog heart cells. *Journal of General Physiology* **83**, 105–131.

MITCHELL, M. R., POWELL, T., TERRAR, D. A. & TWIST, V. W. (1983). Characteristics of the second inward current in cells isolated from rat ventricular muscle. *Proceedings of the Royal Society* B **219**, 447–469.

MITCHELL, M. R., POWELL, T., TERRAR, D. A. & TWIST, V. W. (1984). Ryanodine prolongs Ca-currents while suppressing contraction in rat ventricular muscle cells. *British Journal of Pharmacology* **81**, 13–15.

NAKANISHI, T. & JARMAKANI, J. M. (1984). Developmental changes in myocardial mechanical function and subcellular organelles. *American Journal of Physiology* **246**, H615–625.

NAYLER, W. G. & FASSOLD, E. (1977). Calcium accumulating and ATPase activity of cardiac sarcoplasmic reticulum before and after birth. *Circulation Research* **11**, 231–237.

NILIUS, B., HESS, P., LANSMAN, J. B. & TSIEN, R. W. (1985). A novel type of cardiac calcium channel in ventricular cells. *Nature* **316**, 443–446.

PAGE, E. & BUECKER, J. L. (1981). Development of dyadic junctional complexes between sarcoplasmic reticulum and plasmalemma in rabbit left ventricular myocardial cells. *Circulation Research* **48**, 519–522.

PENEFSKY, Z. (1974). Ultrastructural studies of the site of action of ryanodine on heart muscle. *Pflügers Archiv* **347**, 185–198.

PESSAH, I. N., FRANCINI, A. O., SCALES, D. J., WATERHOUSE, A. L. & CASIDA, J. E. (1986). Calcium–ryanodine receptor complex. *Journal of Biological Chemistry* **261**, 8643–8648.

PESSAH, I. N., WATERHOUSE, A. L. & CASIDA, J. E. (1985). The calcium–ryanodine receptor complex of skeletal and cardiac muscle. *Biochemical and Biophysical Research Communications* **128**, 449–456.

RIOS, E. & BRUM, G. (1987). Involvement of dihydropyridine receptors in excitation–contraction coupling in skeletal muscle. *Nature* **325**, 717–720.

SCHNEIDER, M. F. & CHANDLER, W. K. (1973). Voltage-dependent charge movement in skeletal muscle: a possible step in excitation–contraction coupling. *Nature* **242**, 244–246.

SCHWARTZ, L. M., MCCLESKEY, E. W. & ALMERS, W. (1985). Dihydropyridine receptors in muscle are voltage-dependent but most are not functional calcium channels. *Nature* **314**, 747–751.

SEGUCHI, M., HARDING, J. A. & JARMAKANI, J. M. (1986). Developmental change in the function of sarcoplasmic reticulum. *Journal of Molecular and Cellular Cardiology* **18**, 189–195.

SUTKO, J. L. & KENYON, J. L. (1983). Ryanodine modification of cardiac muscle responses to potassium-free solutions. Evidence for inhibition of sarcoplasmic reticulum calcium release. *Journal of General Physiology* **82**, 385–404.

SUTKO, J. L., WILLERSON, J. T., TEMPLETON, G. H., JONES, L. R. & BESCH JR, H. R. (1979). Ryanodine: Its alterations of cat papillary muscle contractile state and responsiveness to inotropic interventions and a suggested mechanism of action. *Journal of Pharmacology and Experimental Therapeutics* **209**, 37–47.

TSIEN, R. Y. (1980). New calcium indicators and buffers with high selectivity against magnesium and protons. Design, synthesis, and properties of prototype structures. *Biochemistry* **19**, 2396–2404.

VAN GINNEKEN, A. C. G. & JONGSMA, H. J. (1983). Slow inward current in aggregates of neonatal

rat heart cells and its contribution to the steady-state current–voltage relationship. *Pflügers Archiv* **397**, 265–271.

WEBER, A. (1968). The mechanism of the action of caffeine on sarcoplasmic reticulum. *Journal of General Physiology* **52**, 760–772.

YUE, D. T. & MARBAN, E. (1987). Single Ca channel currents carried by Ca and Ba in heart cells: No anomalous mole fraction effect. *Circulation* **76**, suppl. IV, 134.

EXPLANATION OF PLATES

PLATE 1

Ultrastructure of an adult single cardiac myocyte. *A*, low-power view of a single cell. *B*, high-power view of the same cell as in *A*.

PLATE 2

Ultrastructure of a neonatal single cardiac myocyte. *A*, low-power view of a single cell. *B*, high-power view of the same cell as in *A*.

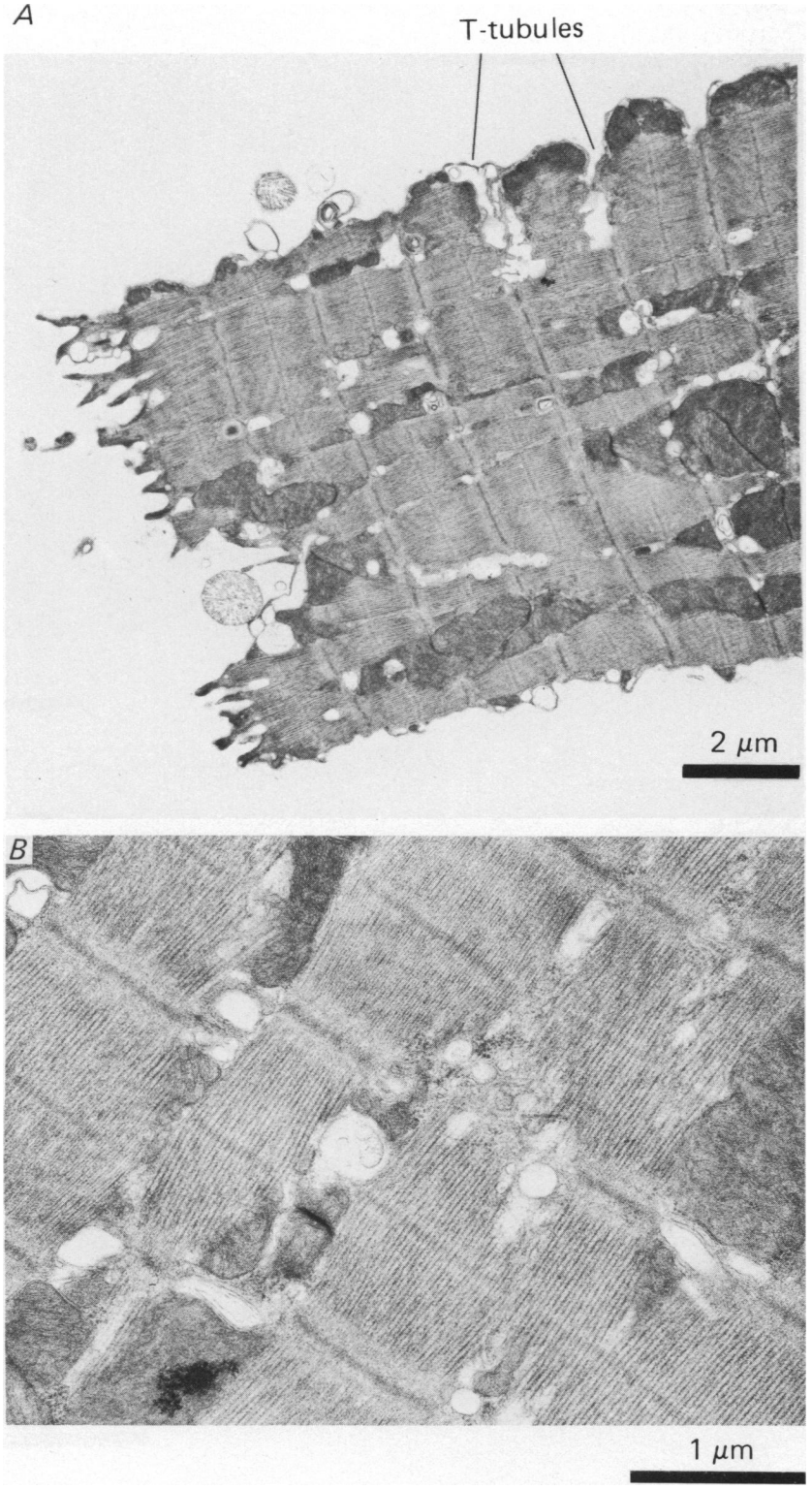
A
T-tubules
2 μm
B
1 μm

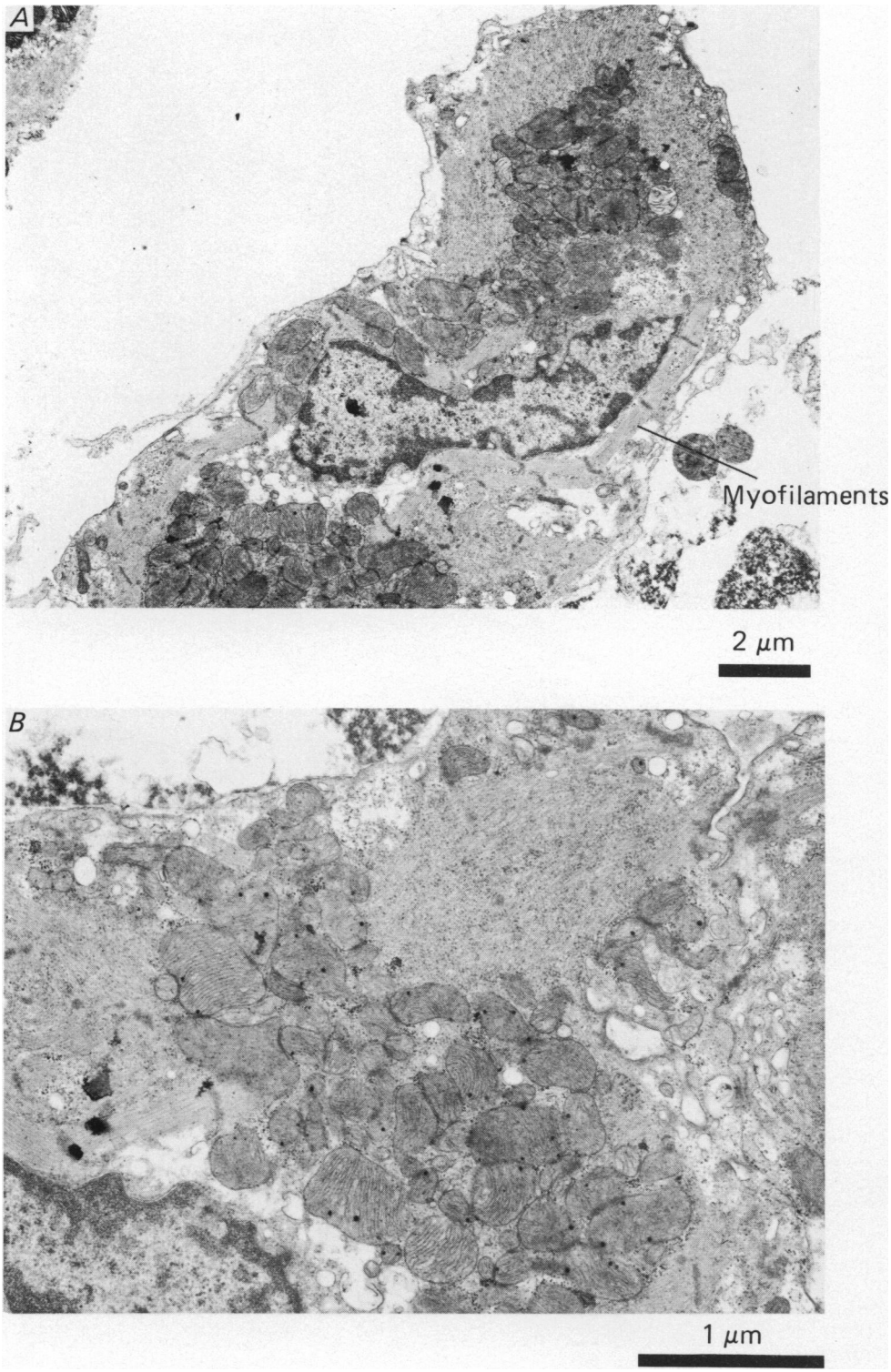
A
Myofilaments
2 μm
B
1 μm